Sea level projections for South Asia

Report on main findings

Benjamin Harrison - benjamin.harrison@metoffice.gov.uk

Reviewed by Joseph Daron and Matthew Palmer

August 2020

ARRCC
Asia Regional Resilience to a Changing Climate

Met Office

UKaid
from the British people

Contents

Executive Summary

As part of the Climate Analysis for Risk Information and Services in South Asia (CARISSA) project, under the Asia Regional Resilience to a Changing Climate (ARRCC) programme, the Met Office is working in partnership with organisations in South Asia to enhance the use of regional climate information to inform adaptation planning. This includes the development of coastal climate services to address the risks of sea level rise that threatens vulnerable coastal communities in the region.

The Met Office recently produced sea level projections for the United Kingdom, as part of the government-funded UK Climate Projections 2018 (UKCP18) project (Lowe et al., 2018). The methods developed for UKCP18 Marine (Palmer et al., 2018a) have since been used to generate sea level projections for tide-gauge locations around the world.

As part of CARISSA, new sea level projections for selected tide-gauge locations in the South Asia region have been produced. 50 tide-gauge locations were selected from the Arabian Sea, Bay of Bengal and Equatorial Indian Ocean regions. The study provides projections for the 21st century, compared to a baseline period of 1986 to 2005, under three future greenhouse gas scenarios (representative concentration pathways RCP2.6, RCP4.5 and RCP8.5), with extended projections to the year 2300.

In the Arabian Sea and Bay of Bengal, projected sea level changes are generally smaller (0.11-0.95 m, likely range across RCPs) compared to projected global average sea level changes (0.29-1.10 m, likely range across RCPs) by the end of the 21st century. The regional differences in sea level rise relative to the global average arise from spatial patterns of regional sea level change due to; loss of terrestrial liquid water mass (land water storage) and glacial isostatic adjustment (GIA). There are north-south gradients in projected sea level change for both regions, with larger changes at locations in the south of these regions. In Equatorial Indian Ocean and far south of the Arabian Sea (e.g. Cochin, India) and Bay of Bengal (e.g. Port Blair, India Andaman Islands), projected sea level changes are larger (0.22-1.20 m, likely range across RCPs by 2100) than projections for global sea level change. Projected changes for locations in the east of the Bay of Bengal (e.g. Port Blair, Indian Andaman Islands, 0.24-0.92 m, likely range across RCPs) are slightly larger than for locations at similar latitudes in the west (Chennai, India, 0.19-0.89 m, likely range across RCPs). For nearly all locations in the Equatorial Indian ocean, the projected changes are slightly

larger than global average sea level changes for RCP2.6, representing 76-117% of the corresponding global changes but become closer to the global average for RCP8.5, representing 80-100% of the corresponding global changes 2081-2100 relative to 1986-2005.

Under all future climate scenarios, there are differences in projected sea level change across the region. For Bangladesh and Pakistan, focal countries for the ARRCC programme, spatial variations in sea level projections arise primarily from differences in the contributions from the Glacial Isostatic Adjustment (the response of land masses to the retreat of ice sheets from the last glacial period) and differences in land water storage changes (net changes from reservoir impoundment and ground water extraction). For India, spatial variations between the northern and southern areas of both coastlines are primarily due to differences in the contributions from the ice sheet component. The rate and extent of melting ice in the Antarctic is the leading source of uncertainty for the 21st century and extended range projections, under all scenarios.

The findings inform our understanding of the differences between projected regional and global sea level changes in the South Asia region. They also provide more relevant information to guide adaptation policy and decision-making. Future work will integrate the projections with local-level contextual information to develop coastal climate services for specific applications.

1. Introduction

1.1 Background and aims

Sea level rise over the coming decades and centuries has been identified as one of the most important risks facing coastal nations and communities (IPCC AR5, Church et al. 2013; SROCC; (Pörtner et al., 2019). Estimates based on tide-gauge records suggest that global mean sea level (GMSL) has risen at a rate of 1.4 mm per year (0.8 to 2.0 mm/year, very likely range) over the period 1901 to 1990 (SROCC, 2019). Since 1993, more accurate information is available from satellite altimeter measurements, and estimates from the period 1993 to 2015 indicate the rate of GMSL has increased by factor of 2.5 to a rate of 3.6 mm per year (Oppenheimer & Glavovic, 2019).The low-lying islands and densely populated coastal areas of South Asia are especially vulnerable to the impacts of sea level rise, such as coastal erosion and increased inundation from tropical cyclone storm surges. Those responsible for formulating and implementing coastal adaptation measures therefore need up-to-date information about observed and projected sea level rise, over a range of temporal-spatial scales.

As part of the Climate Analysis for Risk Information and Services in South Asia (CARISSA) project, under the Asia Regional Resilience to a Changing Climate (ARRCC) programme[1], the Met Office is working in partnership with organisations in South Asia to enhance the use of regional climate information in adaptation policy and planning decisions, focusing on four countries: Afghanistan, Bangladesh, Nepal and Pakistan. The focus of this report is on the presentation and discussion of new projections of mean sea level changes over the 21st century and beyond for selected tide gauge locations across the South Asia region. The projections are generated for three future greenhouse gas representative concentration pathways (RCPs, Meinshausen et al., 2011): RCP2.6, RCP4.5 and RCP8.5.

In previous work under the ARRCC programme, a systematic review of recent[2] scientific literature on sea level rise and coastal adaptation was conducted for

[1] Asia Regional Resilience to Changing Climate (ARRCC) Met Office partnership website: https://www.metoffice.gov.uk/services/government/international-development/arrcc

[2] Literature reviews restricted to publications from the periods 2009-2019 and 2010-2020 for Bangladesh and Pakistan respectively.

Bangladesh (Harrison 2020) and Pakistan (Weeks and Harrison. 2020)[3]. Recent coastal impact and adaptation studies for these countries have generally been based on GMSL projections. Although observed and projected regional mean sea level changes are broadly in line with GMSL change, additional physical processes can result in substantial differences from GMSL at regional (M. D. Palmer et al., 2020) and local scales. Information on regional and local scale sea level change is important for coastal adaptation, seeking to prioritise sections of coastline based on vulnerability to sea level rise impacts (Hinkel et al., 2019).

To address the need for more locally relevant sea level information to inform planning and adaptation policy in Bangladesh and Pakistan, this study details the methods and findings of work to produce new mean sea level projections for locations across the South Asia region. The work described in this report aims to:

1) provide new projections for mean sea level changes at tide gauge locations in the South Asia over the 21st century;

2) assess differences between the GMSL projections and local mean sea level projections at each tide gauge location;

3) estimate contributions from different physical processes to regional sea level change and uncertainty; and,

4) provide an exploratory set of extended projections beyond 2100 to illustrate the potential longer-term changes.

Additional information on the materials and methods used in this study are provided in a separate annex report referred to where relevant, available on the project website[3] above.

Future work in the CARISSA project will integrate these projections with more localised climatic and non-climatic data (e.g. subsidence, erosion and sedimentation) to develop coastal climate services providing decision-relevant information for coastal adaptation planning and coastal risk management.

[3] *Supporting documents :* *https://www.metoffice.gov.uk/services/government/international-development/climate-analysis-for-risk-information--services-in-south-asia-carissa*

1.2 Key findings

- Historical tide gauge records and satellite altimetry measurements show substantial year-to-year and seasonal changes in coastal water level, related to natural variability. This internal variability represents the largest contribution to uncertainty (variance) over the near-term (2021-2040) but uncertainties associated with climate emission scenario and model climate sensitivities become the dominant sources of uncertainty over the remainder of the 21st century and beyond (see section 3.4)
- The 21st century projections for sea level change at tide gauge locations around the Arabian Sea and Bay of Bengal vary with location and climate scenario. For example, at Karachi (Pakistan) and Chittagong (Bangladesh) the projected range of changes for the period 2081-2100 are 0.11-0.49 m, 0.19-0.61 m, 0.32-0.82 m and are 0.17-0.59 m, 0.29-0.68 m, 0.41-0.86 m, for RCP2.6, RCP4.5 and RCP8.5 respectively relative to the baseline period of 1986-2005 (see table 1.2).
- In the Arabian Sea and Bay of Bengal, projected sea level changes are generally smaller than projected global average sea level changes by the end of the 21st century. For example, the range projected changes for 2081-2100 at Karachi and Chittagong represent approximately 41-84%, 55-88%, 64-83% and 79-110%, 94-105%,86-92%, of the corresponding projected global changes for RCP2.6, RCP4.5 and RCP8.5 respectively.
- In contrast for the Equatorial Indian Ocean and far south of the Bay of Bengal (e.g. Port Blair, Indian Andaman Islands) and Arabian Sea (e.g. Cochin, India) projected changes are similar or slightly larger than the global projections. For example, projected changes at Male (Maldives) for the period 2081-2100 are 0.27-0.63 m, 0.34-0.73 m, 0.47-0.95 m and represent approximately 95-107%, 97-105%, 93-98% of the corresponding global changes for the three RCPs.
- The risk of coastal flood events is expected to rise with increasing time-mean sea level, assuming no significant reductions to tropical cyclone frequency, intensity or changes to tropical cyclone trajectories in Arabian Sea and Bay of Bengal.
- Exploratory time-mean sea level projections to 2300 suggest that sea level in South Asia will continue to rise under all climate change scenarios. There is a much larger degree of unquantified uncertainty associated with sea-level

information on these extended time horizons. Therefore, these projections should be considered as illustrative of potential future changes.

	Range of sea-level change by 2100 (metres)		
	RCP2.6	RCP4.5	RCP8.5
Chittagong	0.17 – 0.62	0.28 – 0.68	0.41 – 0.86
Khulna (Hiron Point)	0.15 – 0.61	0.28 – 0.67	0.39 - 0.84
Kolkata (Diamond Harbour)	0.14 – 0.58	0.26 – 0.64	0.37 – 0.81
Mumbai (Princess Dock)	0.19 – 0.55	0.27 – 0.68	0.40 – 0.86
Karachi	0.11 – 0.49	0.19 – 0.61	0.32 – 0.81
Gwadar	0.17 – 0.51	0.25 – 0.63	0.37 – 0.85

Table 1.2. *The 5th – 95th percentile (or in IPCC calibrated language, "likely") range of projected sea level changes at a sample of South Asia location, for the period 2081-2100 relative to the baseline period of 1986-2005.*

1.3 Caveats and limitations

- The 21st century projections presented in this report are based on CMIP5 climate models and RCP scenarios. Results are therefore subject to any limitations of the underlying model ensembles and assumed climate change scenarios.
- The projection ranges are based on the 5th to 95th percentiles of the underlying model distributions. There may be a greater than 10% chance that the real-world response lies outside the 5th to 9th percentile range and this likelihood cannot be accurately quantified. Substantial additional sea level rise, associated primarily with dynamic ice discharge from the West Antarctic Ice Sheet (DeConto & Pollard, 2016; Edwards et al., 2019), cannot be ruled out. We recommend that coastal adaptation decision makers use multiple strands of evidence, including observed sea level records and high-end scenarios when assessing vulnerabilities to future extreme water levels.
- The extended time-mean sea level projections have much lower confidence than the 21st century projections. These projections can be considered as sensitivity studies and should not be interpreted as showing the full range of post 2100 behaviour, or the most likely behaviour. The contribution to sea-level rise from Antarctic dynamic discharge is even more uncertain on these time horizons, with some studies suggesting several additional metres of sea level rise by 2300 under RCP8.5 (SROCC, 2019).

2. Sea level rise processes and projections

Section summary

Changes in sea level arise from a variety of geophysical processes acting on different spatial-temporal scales. GMSL rise occurs primarily from thermal expansion of seawater and the addition of water to the oceans from the loss of land-based ice and water. Changes in land-based ice and water storage result in differing spatial patterns of regional sea level change, associated with changes in the Earth's gravitational field and other effects. Local changes in seawater density and ocean circulation also give rise to spatial differences, which vary markedly among different climate models and is therefore introduce uncertainties. In addition, the ongoing response of the Earth system to the last deglaciation brings about a specific spatial pattern of regional sea-level change for South Asia driven by vertical land motion. At local scales, the impacts of sea level change typically occur due to extreme sea level events. Deviations from the regional mean sea level can arise from extreme wave conditions, tropical storm surges and local tide. All future projections of regional mean sea level changes are rooted in, or traceable to CMIP5 climate model simulations under the RCP climate change scenarios. A key uncertainty for future sea level projections across the world is the potential for accelerated sea level rise from the loss of land-based ice, particularly from Greenland and Antarctica. Despite recent advances in knowledge, for example on the potential collapse of the West Antarctic ice sheet, there is a critical need for close monitoring and improved modelling of ice sheet dynamics to reduce this key uncertainty.

2.1 The sea level "jigsaw puzzle"

Changes in sea level occur due to a broad range of geophysical processes that act on different spatial-temporal scales. Like the pieces of a jigsaw puzzle, different processes combine and interact to form the whole picture. In this section we present a schematic (figure 2.1) of the different sea level components that are included in the new sea level projections for South Asia, discussing their different terms and interactions.

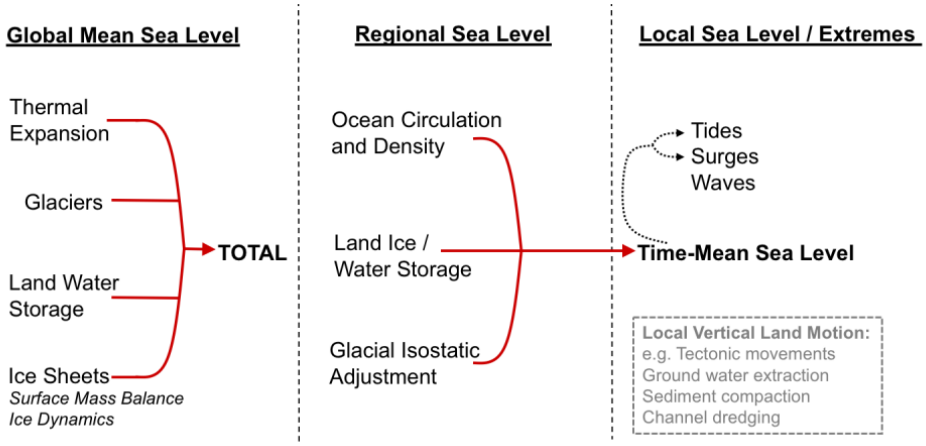

Figure 2.1: *The sea level "jigsaw puzzle", summarising the major contributors to changes in: global time-mean sea level (left-hand column); regional sea level (middle column), local sea-level and extreme sea-level (right hand column). The potential interaction between time-mean sea-level tide and surge characteristics is indicated by the dashed black lines. The grey text highlights some of the non-climate processes that can give rise to sea-level change, such as vertical land motion. Reproduced from (Palmer et al., 2018a)*

Changes in GMSL (figure 2.1, left column) arise due to either: (i) changes in the average ocean density (e.g., if the ocean becomes less dense the volume of water increases and GMSL rises); or (ii) a change in global ocean mass due to the addition or removal of water. For GMSL, changes in density are overwhelmingly dominated by thermal expansion; i.e. the tendency for seawater to become less dense as the temperature increases (e.g. Griffies et al., 2014). Changes in sea level due to density changes are referred to as steric changes. Under anthropogenic climate change, freshwater input to the ocean arises from loss of land-based ice from the Greenland and Antarctica ice sheets and mountain glaciers. Following IPCC AR5 (Church et al. 2013) and the UKCP18 Marine Projections (M. Palmer et al., 2018), the sea level projections for South Asia include both surface mass balance (i.e. the balance between accumulated snowfall and ice melt) and ice dynamics (i.e. changes in the rate of discharge in active ice flows) for each of the ice sheets. Finally there can be additional contributions to sea level rise (both positive and negative) due changes in mass of non-frozen land-based water, through groundwater extraction and impoundment of water (by dams and reservoirs) that make a substantial contribution to GMSL change (John A. Church et al., 2011; Dieng et al., 2015; Wada et al., 2012, 2016).

For regional sea level changes, several additional processes come into play (figure 2.1, central column). Firstly, changes in local seawater density and/or ocean circulation leave their imprint in the shape of the sea surface (Slangen et al., 2014). While temperature effects dominate density changes for GMSL, at the regional scale both

changes in temperature and salinity are important factors (Llovel & Lee, 2015; J.A Lowe & Gregory, 2005; Pardaens et al., 2011). Due to differing responses among climate models (Pardaens et al., 2011; Slangen et al., 2014), the spatial pattern of change associated with the ocean circulation and density in highly uncertain. Following the nomenclature of (Gregory et al., 2019) we refer to the combined effect of changes in global thermal expansion (steric changes) and regional ocean circulation (dynamic changes) as “sterodynamic” sea level change.

Secondly, changes in land-based ice and water storage are also associated with spatial patterns of regional sea level change. These spatial patterns depend on the geographic distribution of the mass changes and arise from: (i) the solid Earth response to changes in local mass loading; (ii) the effect of mass redistribution on the Earth’s gravity field; and (iii) the combined effect of (i) and (ii) on the Earth’s rotation (Tamisiea & Mitrovica, 2011). In nomenclature of Gregory et al. 2019 the spatial patterns will be referred to as gravitation, rotation, deformation (GRD) patterns. Following Palmer et al. (2018a) The projections in presented in this report use GRD estimates from two different model solutions. Details on these GRD estimates can be found in section A1.3 (supporting materials and methods report)

Thirdly, the ongoing response of the Earth system to the last deglaciation (which ended approximately 10,000 years ago) – referred to as glacial isostatic adjustment (GIA) – gives rise to a spatial pattern of sea level change across the region with peak magnitudes of approximately – 0.5 to + 1 mm per year (see section A1.4, supporting materials and methods report). This pattern is characterised by a negative contribution to sea level rise near the sub-continent landmass and positive contribution to sea level rise towards the equator and interior of the Arabian Sea and Bay of Bengal sub-basins. Due to the adjustment timescales associated with GIA, the rates of change are assumed to be constant over the time horizons considered in the sea level projections.

The superposition of the different spatial varying elements (i.e. sterodynamic sea level change, GRD, GIA) described above, determine the sea level change for a given location in the sea level projections (see section A2.2, supporting materials and methods report). In addition to the climate change signal, coastal decision makers should be aware of the substantial interannual variation in time-mean sea level, as evidenced by studies of water level records in the region (Becker et al., 2020; Han et al., 2019; Nidheesh et al., 2019). The future evolution of regional and local sea level

will have contributions from the climate change signal represented by time-mean sea level projections and this background variability. For this reason, information on the processes and spatial patterns of coastal sea level variability will need to be considered alongside the time-mean sea level projections.

For local scale changes in mean sea level (figure 2.1, right column), non-climate physical process such as subsidence and tectonic uplift can contribute to changes in the local mean sea level relative to the sea floor[4] (hereafter referred to as relative sea level change) through vertical land movement (Gregory et al. 2019). The sea level projections for the tide gauge locations in this study are based on changes to relative sea level but do not account for vertical land motion due "non-climatic" processes, apart vertical land contributions from GIA. The rate of vertical land movement due to non-climatic processes can be comparable to, or greater than climate-driven trends in GMSL (or local mean sea level) but often highly localised. For example, subsidence rate (negative vertical land motion) estimates for sections of the Bangladesh coastline (Becker et al., 2020; Brammer, 2014; Higgins et al., 2014), and tectonic uplift (positive vertical) estimates for the Balochistan coast in Pakistan (Lahijani et al., 2019) are reported to be comparable to observed mean sea level rates. However, in general subsidence rates are not well known, with estimates ranging from 2-18 mm/yr. for the Ganges-Brahmaputra delta (Higgins et al., 2014; Pethick & Orford, 2013). While for Pakistan there is similar uncertainty regarding the effects of tectonic uplift on relative sea level, since the only long duration sea level records are from Karachi on the tectonically less active Sindh coastline (Kahn et al. 2020, Weeks and Harrison. 2020).

Many of the most severe and earliest effects of sea level rise will be experienced during extreme high-water events, which are usually associated with high tides and combined with storm surges and may involve overtopping due to extreme wave heights. Although the projections in this report do not consider the potential changes to local tides, wave climate or atmospheric storms, previous studies have indicated that dominant driver of changes in sea level extremes is from changes to time mean sea level (Cannaby et al., 2016; Howard et al., 2019; Oppenheimer & Glavovic, 2019; M. Palmer et al., 2018). Changes to local extreme sea level can arise from interactions between changes in the local time-mean sea level, tide and surge characteristics because of the influence

[4] *Note: Relative Sea level change refers to "the change in local mean sea level relative to a local solid surface" (Gregory et al. 2019)*

of water depth on the tide and surge (Pethick & Orford, 2013). These effects can be examined by considering how past extreme events might play out given future increases in local time-mean sea level, although this topic is beyond the scope of this initial study.

2.2 Overview of model datasets

The sea level projections are derived from climate model simulations from the Coupled Model Intercomparison Project Phase 5 CMIP5, (Taylor et al., 2012). These models formed the basis of the climate projections presented in the IPCC AR5 (Church et al. 2013) and used in UKCP18 (M. Palmer et al., 2018a; M. D. Palmer et al., 2020). While there was a substantial improvement from CMIP3 to CMIP5 in the representation of mean sea level (Landerer et al., 2014; Meehl et al., 2007), differences between CMIP5 and the successor CMIP6 (Eyring et al., 2016) simulations are less significant and mainly found in the Southern Hemisphere at mid to high latitudes (Lyu et al., 2020).

Sea level projections are provided for three RCPs: RCP2.6, RCP4.5, and RCP8.5. We do not include RCP6.0 because the scenario exhibits a similar GMSL at 2100 to RCP4.5 and has poorer data availability in the CMIP5 database than the other scenarios.

2.3 Potential for accelerated sea level rise from Antarctic ice loss

A key source of uncertainty in projections of global mean sea level at the end of the 21st century is the contribution to sea level rise from the loss of ice stored in the Antarctic and Greenland ice sheets. SROCC Summary for Policymakers (SROCC SPM) states that: “the uncertainty at the end of the century is mainly determined by the ice sheets, especially in Antarctica” (Pörtner et al., 2019). Unlike the Greenland ice sheet, recent contributions to sea level rise from the Antarctica ice sheet have been dominated by dynamical ice loss processes, rather than changes in surface mass balance (Pörtner et al., 2019), particularly for the West Antarctic ice sheet. The West Antarctica ice sheet is a predominantly marine-terminating ice sheet, where ice mass input to the ocean is governed primarily by ice flow processes rather than the surface mass balance (between snow accumulation and ice melt) that dominates for the East Antarctic Ice Sheet.

The large uncertainty in the contribution from the Antarctic Ice sheet means that we cannot rule out the potential for sea level in excess of the range in sea level projections described in this report. The statement from SROCC Summary for Policymaker in this regard is:

“Processes controlling the timing of future ice-shelf loss and the extent of ice sheet instabilities could increase Antarctica’s contribution to sea level rise to values substantially higher than the likely range on century and longer time-scales” (Pörtner et al., 2019).

Despite the progress in understanding the processes governing ice sheet loss and ice sheet instabilities since IPCC AR5, it remains difficult to simulate ice sheet processes and their interactions with the ocean, atmosphere and underlying bedrock (Oppenheimer & Glavovic, 2019). Hence, the potential for additional sea level rise (i.e. beyond the likely range 0.03-0.28m for 2100) from Antarctic dynamical ice loss represents a source of unquantified uncertainty (referred to as “deep uncertainty”). This deep uncertainty arises from “lack of knowledge about processes, and disagreement about appropriate models and probability distributions for representing uncertainty” (Pörtner et al., 2019; Rohmer et al., 2019).

The deep uncertainty that arises from the dynamical ice sheet contribution to sea level rise means that it is not possible to unambiguously define an upper bound for sea level rise for the 21st century. This means it is not possible to unambiguously define or assign probabilities to a “worst-case”. However, recognising the demand for information on sea level rise beyond the “likely-range” several authors have proposed ways to construct so called “high-end” scenarios for decisions makers interested in exploring potential a wider range of potential damage costs due to sea level rise beyond the likely range or prospective planning costs required for adaptation measures that are tolerant against a wider range of sea-level rise scenarios (Kopp et al., 2019; Stammer et al., 2019).

3. 21st Century Projections

Section summary

The 21st century time-mean sea level projections for South Asia follow the methodology developed for UKCP18, which built upon the materials and methods described in the IPCC AR5. Coastal sea level projections around the region show substantial variations associated with both the RCP climate change scenario and geographic location. In general, greater sea level rise is projected for southern sections of the Arabian Sea and Bay of Bengal coastlines, where values are similar or slightly less than GMSL. In contrast for the Equatorial Indian Ocean and far-south of Arabian Sea and Bay of Bengal, values are in-line with or slightly larger than global average. In the north and central areas of the Arabian Sea and Bay of Bengal, sea level rise projections are slightly lower than GMSL, with the lowest projected changes found along the Pakistan coast. For the major ports in Pakistan (Karachi, Gwadar) and Bangladesh (Chittagong), projections at 2100 range from approximately 0.11-0.59 m (Karachi and Chittagong under RCP2.6) to 0.32-0.86 m (Karachi and Chittagong under RCP8.5). The lower rates of sea level rise for the Arabian Sea and Bay of Bengal relative to the global average is due to the regional GRD patterns of sea level change associated with the loss of terrestrial water mass over the Indian sub-continent land mass. Coastal sea level variability is an important additional consideration, particularly for planning time-horizons that limited to a few decades.

3.1 Projections of time-mean sea level change

In this section we present the 21st century projections of changes in time-mean sea level for locations across South Asia. Details on the data sources and methods are presented in sections A1 and A2 respectively, with extended discussion on the projections provided in section A3 (supporting materials and methods report).

The projections of 21st century sea level change focus on the coastlines of the Arabian Sea and Bay of Bengal, and equatorial Indian Ocean. The tide gauge locations for sites used in the study from these regions are shown in figures 3.1a-c respectively. Projections for tide gauge sites use the nearest model grid box to the tide gauge location provided by the Permanent Service for Mean Sea Level (PSMSL), in each of the 21 CMIP5 models (see figures A3.1 to A3.3 in the supporting materials and methods report for the location of the grid-points used in each CMIP5 model).

***Figure 3.1a**: Arabian Sea coastal sites that are included in the projected changes in time mean sea level, selected from tide gauge stations available on the Permanent Service for Mean Sea Level (PSMSL).*

***Figure 3.1b**: Bay of Bengal coastal sites that are included in the projected changes in time mean sea level, selected from tide gauge stations available on the Permanent Service for Mean Sea Level (PSMSL).*

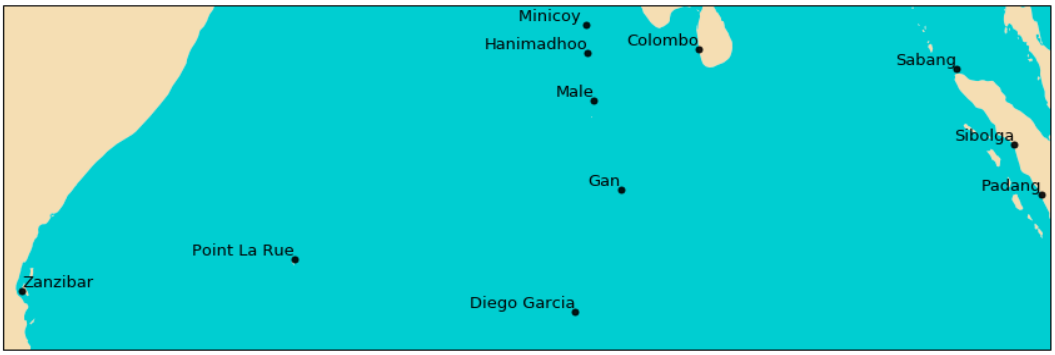

***Figure 3.1c**: Equatorial Indian Ocean coastal sites that are included in the projected changes in time mean sea level, selected from tide gauge stations available on the Permanent Service for Mean Sea Level (PSMSL).*

In this study, time-mean sea level is defined as the annual average baseline water level upon which the drivers of sea level extremes – such as tides, surges and waves – are superimposed. Projections of time-mean sea level are presented as yearly values over the 21st century. We present ranges of future sea level rise for the three RCP scenarios based on the 5th and 95th percentiles of the underlying process-based model projections. IPCC AR5 referred to this as the "likely range" based on their expert judgement that there was a 2/3 chance of sea level rise falling within this model range for a given scenario. The UKCP18 interpretation, used in this report is that there may be a greater than 10% chance that the real-world response lies outside these ranges and that this likelihood cannot be accurately quantified.

In the following section, we present projections of GMSL and compare the results with projections presented in IPCC AR5 and SROCC. Projections for locations in the Arabian Sea, Bay of Bengal and north equatorial Indian Ocean are derived from the GMSL projections and are presented in section 3.3. The relative importance of contributions from different physical to regional sea level change are discussed in section 3.4.

3.2 Global sea level projections

The GMSL projections presented in this section and used as a basis for the South Asia projections are based on those used for the UK sea level projections in the UKCP18 Marine Report (Palmer et al. 2018a) (figure 3.2). The projections differ slightly from the IPCC AR5 projections by the inclusion of updated estimates for the contribution to sea level rise from Antarctica ice dynamics, following Levermann et al (2014). The updated Antarctica ice dynamics contribution systematically increases the projections and raises the values of the 95th percentile range (i.e. the upper bound of the likely range).

The global projections used in this report show similar values at 2100 to global projections from SROCC across RCPs (see table 3.1) and IPCC AR5 but span a larger range (figure 3.2). For RCP2.6 and RCP4.5 the central estimate for projected changes at 2100 are broadly in-line with those from SROCC and IPCC AR5. The updated contribution for Antarctic dynamical ice loss, results in a higher central estimate at 2100 relative to AR5 for the global projections in this study but lower than the central estimate from the SROCC, which is also primarily determined by the Antarctic component (Palmer et al., 2020).

	Global time-mean sea level rise at 2100 (metres)	
Scenario	**Present Study**	**IPCC SROCC**
RCP2.6	0.28 – 0.65	0.28 – 0.59
RCP4.5	0.37 – 0.78	0.38 – 0.72
RCP8.5	0.55 –1.11	0.61 – 1.11

Table 3.1: *Summary of the projected global sea level change at 2100 used in the present study (Palmer et al., 2020) and projections (SROCC).*

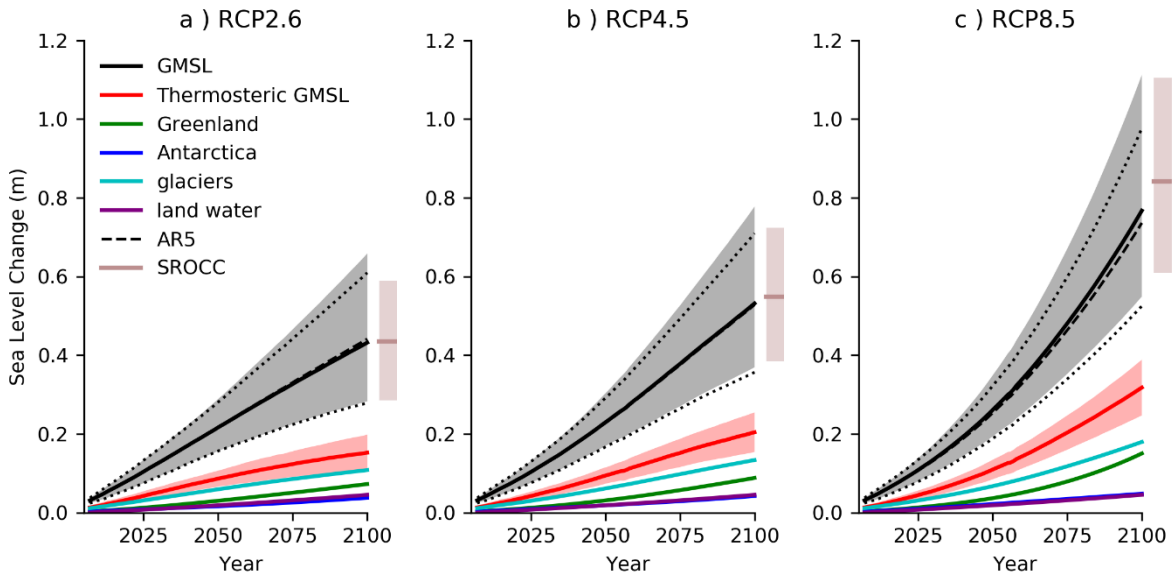

Figure 3.2: *Global time-mean sea level (GMSL) projections for the 21st century adapted from Palmer et al* (2020)*, including components indicated in the figure legend. The shaded regions indicate the range of projections for the total GMSL rise and from global mean thermosteric sea level rise, from ocean thermal expansion. Also shown are total sea level changes from projections presented in IPCAR5 (Church et al. 2013) with the range indicated by the dotted lines and those from SROCC (Oppenheimer et al. 2019) with the range indicated by the brown boxplots*.

3.3 Sea level projections for South Asia

The coastal sea level projections presented in this section are derived from the GMSL projections presented in the previous section 3.2. The methods are described further in section A2 (supporting materials and methods report). The procedure takes account of geographical patterns of sea level change from changes in land-based ice and water mass (e.g. Tamisiea and Mitrovica, 2011; Slangen et al. 2014) and patterns of strerodynamic sea level change (e.g. Cannaby et al. 2016; Palmer et al. 2020). The final component for the regional projections is an estimate of regional sea level changes associated with the ongoing response of the solid Earth to the last de-glaciation (referred to as glacial isostatic adjustment). This combination of factors results in geographical variations in projected sea level changes over South Asia region.

In general, there is larger uncertainty for local sea level projections than for GMSL projections, as indicated by the larger range of values for a given scenario. This increased uncertainty, stems partly from local ocean circulation and density changes (sterodynamic changes), which represents the dominant driver of sea level change for South Asia region (section 3.4). In contrast the local GRD contribution from land-based ice and water mass changes are highly consistent across different GRD models (Palmer et al., 2020).

The time-evolution of the South Asia sea level projections have very similar time evolution to the corresponding GMSL time series (figures 3.2). For the both the Arabian Sea and Bay of Bengal coastlines, the average total sea level rise is slightly lower than for GMSL across all scenarios. The remoteness of South Asia from the Greenland and Antarctica ice sheets means that the ice sheet contribution to regional sea level rise shows similar patterns for both domains. The spatial patterns are characterised by a weak north-south gradient with larger sea level changes found at southern locations, where projected changes are closer to the global average (see also section A2.2, supporting materials and methods report). In addition, the range for the South Asia coastal sea level projections is larger than for the GMSL time series, owing to the additional uncertainty associated with the physical processes for sea level rise at regional scales.

Arabian Sea:

The sea level changes for the Arabian Sea for the three RCP scenarios used in this study are summarised in table 3.3, figures 3.3 and 3.4 show plots for RCP2.6 and RCP8.5. Projected changes for locations in the Arabian Sea are generally lower than the global average, across RCP scenarios over the 21st century. We see a basin wide trend of larger sea level changes in the north, compared to the south and for the north of the region, larger changes in the west compared to east. For example, larger projected changes at Gwadar (figure-3.3c) than at Karachi (figure-3.3a) which are located at west and east Pakistan, respectively. These zonal gradients are mainly seen at the lower end of the distributions for RCP2.6 and arise from GRD spatial patterns of change associated with the loss of terrestrial water mass over South Asia, in the land water storage component (see section 3.4 and supporting methods and materials).

2061-2080	RCP2.6	RCP4.5	RCP8.5
Karachi	0.11-0.37	0.16-0.44	0.22-0.53
Cochin	0.20-0.46	0.24-0.52	0.31-0.60
Gwadar	0.15-0.39	0.20-0.46	0.26-0.55
Masirah	0.16-0.41	0.22-0.48	0.28-0.58
Ormara	0.14-0.39	0.19-0.46	0.26-0.54
Vanidar	0.13-0.38	0.17-0.45	0.24-0.53
Mumbai	0.17-0.43	0.21-0.49	0.28-0.56
Okha	0.13-0.38	0.17-0.45	0.24-0.53
Bhaunagar	0.11-0.39	0.15-0.45	0.23-0.52
Salalah	0.17-0.43	0.22-0.48	0.29-0.59
Djibouti	0.20-0.46	0.24-0.51	0.31-0.62
Kandla	0.14-0.40	0.17-0.47	0.23-0.55
Veraval	0.14-0.41	0.19-0.47	0.26-0.55
Aden	0.18-0.44	0.22-0.49	0.30-0.59
Muscat	0.16-0.41	0.22-0.47	0.27-0.56
Mangalore	0.18-0.44	0.22-0.50	0.29-0.58
Chabahar	0.15-0.39	0.20-0.46	0.26-0.55
Mormugao	0.17-0.44	0.21-0.50	0.28-0.57

2081-2100	RCP2.6	RCP4.5	RCP8.5
Karachi	0.11-0.49	0.19-0.61	0.32-0.82
Cochin	0.24-0.6	0.31-0.72	0.45-0.92
Gwadar	0.17-0.51	0.25-0.63	0.37-0.85
Masirah	0.19-0.54	0.28-0.66	0.4-0.88
Ormara	0.17-0.51	0.24-0.63	0.37-0.84
Vanidar	0.14-0.5	0.21-0.62	0.34-0.82
Mumbai	0.2-0.56	0.27-0.67	0.41-0.87
Okha	0.14-0.5	0.21-0.62	0.34-0.82
Bhaunagar	0.12-0.51	0.19-0.62	0.33-0.81
Salalah	0.21-0.56	0.28-0.66	0.41-0.91
Djibouti	0.24-0.6	0.31-0.7	0.44-0.95
Kandla	0.16-0.52	0.21-0.64	0.33-0.85
Veraval	0.16-0.53	0.24-0.65	0.38-0.85
Aden	0.22-0.57	0.29-0.67	0.43-0.91
Muscat	0.19-0.53	0.28-0.65	0.4-0.85
Mangalore	0.21-0.57	0.28-0.69	0.42-0.89
Chabahar	0.17-0.51	0.25-0.63	0.38-0.85
Mormugao	0.2-0.57	0.27-0.68	0.41-0.88

Table 3.3: *Projected ranges of sea level rise for Arabian Sea locations over the periods 2061-2080 (left) and 2081-2100 (right) under RCP2.6, RCP4.5 and RCP8.5 relative to a baseline period of 1986-2005.*

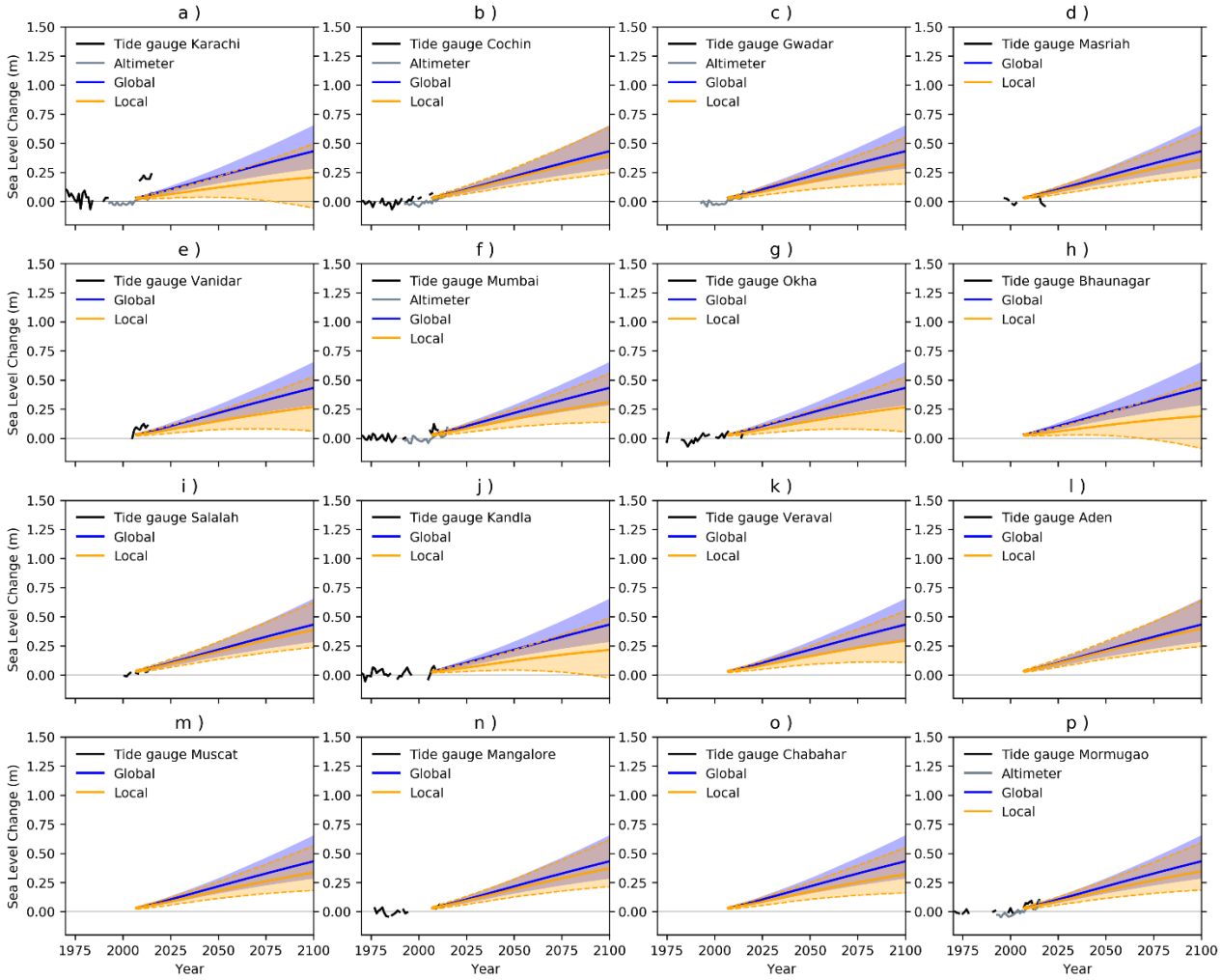

Figure 3.3: *21st century sea level projections for RCP2.6 at tide gauge locations in the Arabian Sea based and projected GMSL changes. Solid lines indicate the central estimate, shaded areas indicate the 5th - 95th percentile range for projected local (yellow) and global (blue) changes.*

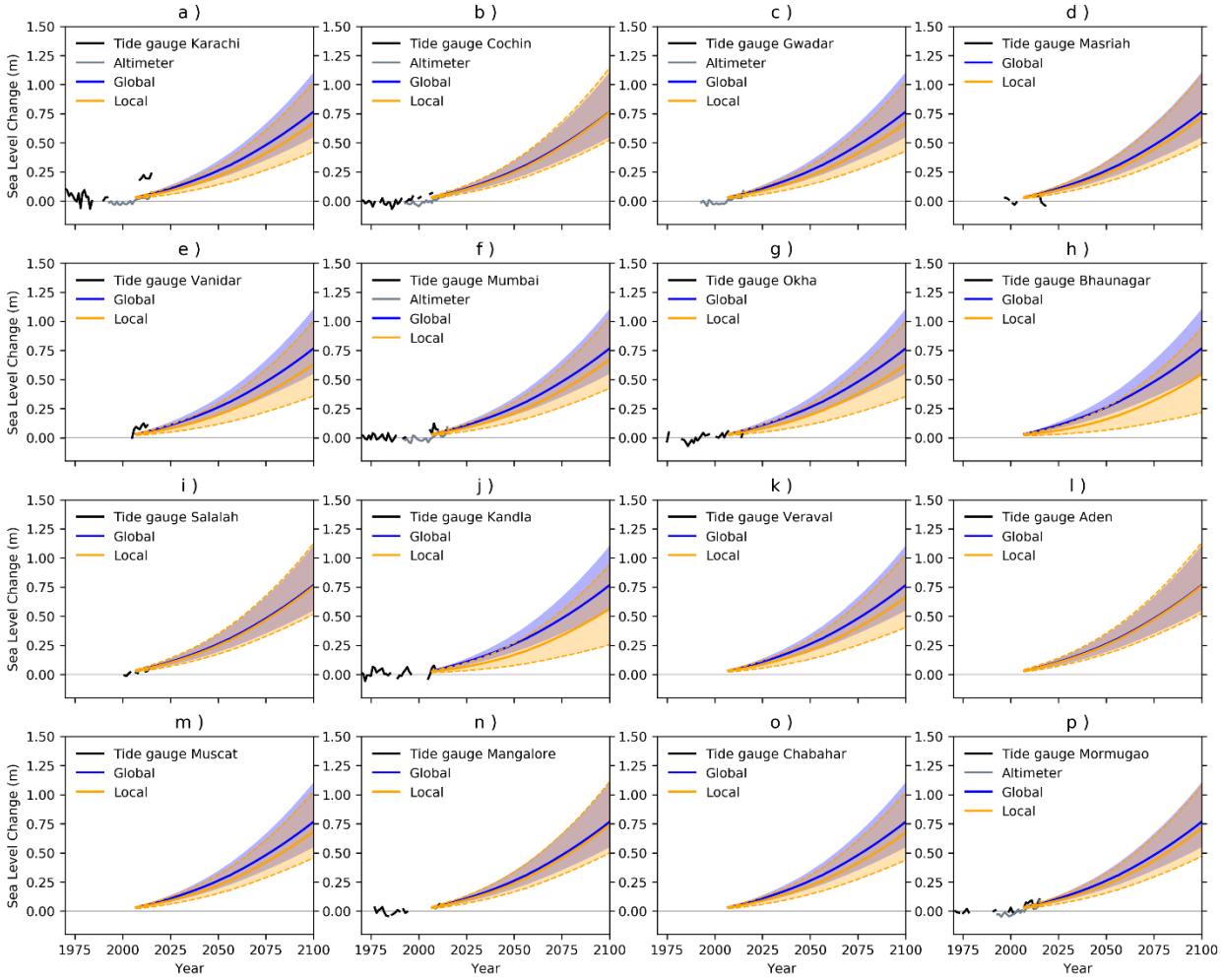

Figure 3.4: *21st century sea level projections for RCP8.5 at tide gauge locations in the Arabian Sea based and projected GMSL changes. Solid lines indicate the central estimate, shaded areas indicate the 5th - 95th percentile range for projected local (yellow) and global (blue) changes.*

Bay of Bengal:

The projected changes for the Bay of Bengal are shown in table 3.4, where we see the same trend of larger sea level changes at equatorward locations. In contrast to the Arabian Sea however, projected changes for the Bay of Bengal are slightly larger in the east. This can be seen in the larger changes at Port Blair in the east of the Bay of Bengal, than at Nagapattinam (figures 3.5,3.6 panels (b) and (j) respectively). Zonal gradients for projected sea level change are smaller than the meridional gradients and mainly seen at the lower end of the distribution for RCP2.6 (figure 3.5) and less evident for RCP8.5 (figure 3.6).

2061-2080	RCP2.6	RCP4.5	RCP8.5
Coxs Bazaar	0.14-0.48	0.23-0.49	0.28-0.56
Port Blair	0.19-0.51	0.26-0.53	0.32-0.6
Visakhapatnam	0.13-0.46	0.21-0.49	0.27-0.54
Paradip	0.13-0.46	0.22-0.49	0.27-0.54
Teknaf	0.13-0.48	0.23-0.5	0.28-0.56
Gangra	0.12-0.46	0.21-0.48	0.27-0.54
Dmnd Harbour	0.11-0.45	0.2-0.47	0.26-0.52
Chennai	0.16-0.48	0.23-0.52	0.29-0.58
Rangoon	0.15-0.48	0.23-0.5	0.28-0.56
Nagapattinam	0.16-0.47	0.23-0.51	0.29-0.58
Sagar	0.13-0.44	0.18-0.5	0.23-0.58
Khal Ten	0.17-0.42	0.19-0.48	0.23-0.58
Tuticorin	0.19-0.46	0.24-0.52	0.31-0.6
Khepupara	0.13-0.47	0.22-0.49	0.27-0.55
Nancowry	0.2-0.51	0.26-0.53	0.32-0.6
Akyab	0.14-0.48	0.23-0.5	0.28-0.55
Haldia	0.11-0.45	0.2-0.47	0.26-0.52
Chittagong	0.14-0.48	0.23-0.5	0.28-0.56
Hiron Point	0.12-0.47	0.22-0.49	0.27-0.55
Moulmein Two	0.18-0.45	0.21-0.51	0.26-0.6
Charchanga	0.13-0.47	0.22-0.49	0.27-0.55
Ko Taphao Noi	0.18-0.5	0.25-0.53	0.3-0.59

2081-2100	RCP2.6	RCP4.5	RCP8.5
Coxs Bazaar	0.17-0.62	0.3-0.68	0.4-0.86
Port Blair	0.24-0.66	0.34-0.73	0.45-0.92
Visakhapatnam	0.16-0.6	0.27-0.68	0.39-0.84
Paradip	0.16-0.6	0.28-0.67	0.39-0.84
Teknaf	0.17-0.62	0.29-0.68	0.4-0.85
Gangra	0.15-0.6	0.28-0.66	0.38-0.83
Dmnd Harbour	0.14-0.58	0.26-0.64	0.37-0.81
Chennai	0.19-0.62	0.29-0.71	0.43-0.89
Rangoon	0.19-0.62	0.29-0.69	0.41-0.86
Nagapattinam	0.2-0.61	0.3-0.71	0.42-0.89
Sagar	0.16-0.57	0.24-0.68	0.33-0.89
Khal Ten	0.2-0.55	0.25-0.66	0.34-0.89
Tuticorin	0.24-0.6	0.31-0.71	0.45-0.93
Khepupara	0.16-0.61	0.28-0.67	0.39-0.84
Nancowry	0.24-0.66	0.34-0.73	0.46-0.92
Akyab	0.18-0.62	0.29-0.68	0.41-0.85
Haldia	0.14-0.58	0.26-0.64	0.37-0.81
Chittagong	0.17-0.62	0.29-0.68	0.41-0.86
Hiron Point	0.15-0.61	0.28-0.67	0.39-0.84
Moulmein Two	0.22-0.59	0.28-0.7	0.37-0.92
Charchanga	0.16-0.6	0.28-0.67	0.39-0.84
Ko Taphao Noi	0.22-0.65	0.33-0.73	0.44-0.91

Table 3.4: *Projected ranges of sea level rise Bay of Bengal locations over the periods 2061-2080 (left) and 2081-2100 (right) under RCP2.6, RCP4.5 and RCP8.5 relative to a baseline period of 1986-2005*

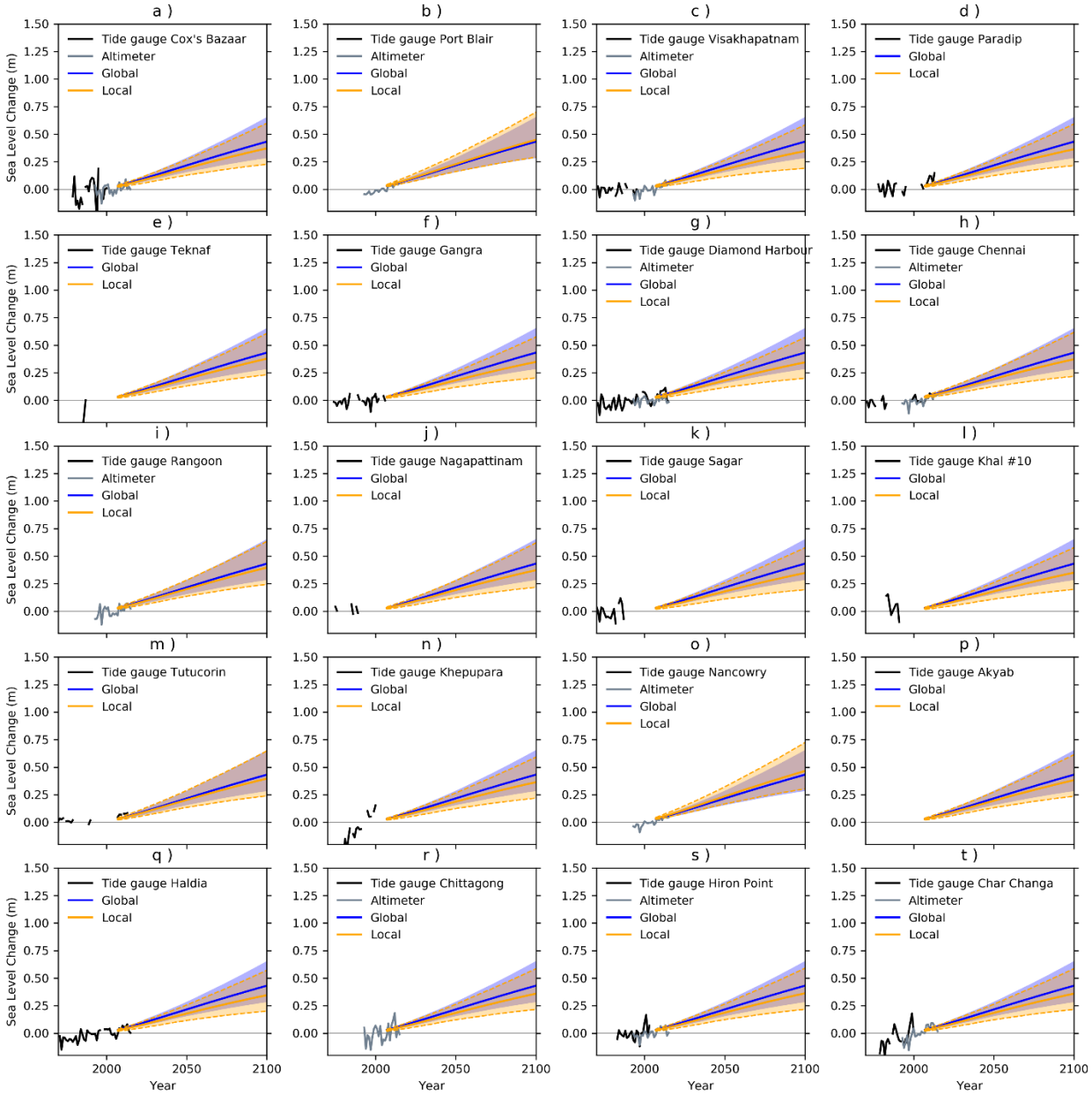

Figure 3.5: *21st century sea level projections for RCP2.6 at tide gauge locations in the Bay of Bengal based and projected GMSL changes. Solid lines indicate the central estimate, shaded areas indicate the 5th - 95th percentile range for projected local (yellow) and global (blue) changes.*

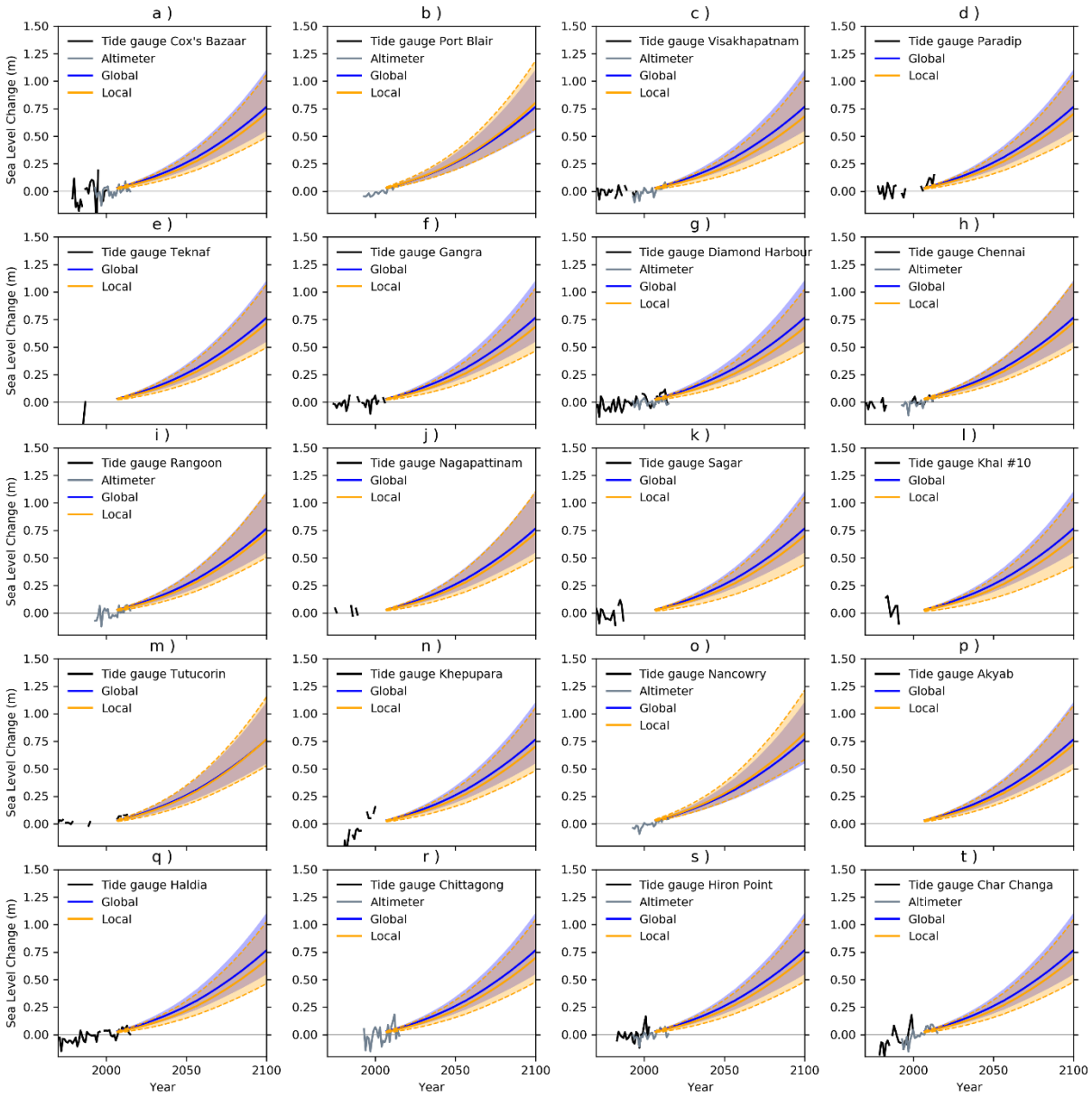

Figure 3.6: *21st century sea level projections for RCP8.5 at tide gauge locations in the Bay of Bengal based and projected GMSL changes. Solid lines indicate the central estimate, shaded areas indicate the 5th - 95th percentile range for projected local (yellow) and global (blue) changes.*

Equatorial Indian Ocean

In the equatorial Indian ocean projections are broadly in line with the global average projections, although slightly larger for the 50th and 95th percentile range for RC2.6 (figure 3.7) but closer to the global average under RCP8.5 (figure 3.8). The projected changes for the equatorial Indian ocean are summarised in table 3.5, which also includes locations in the southern hemisphere to assess if the observed trend of larger rates in the southern Indian continues through the 21st century.

2061-2080	RCP2.6	RCP4.5	RCP8.5
Point La Rue	0.21-0.53	0.25-0.54	0.34-0.65
Padang	0.17-0.49	0.24-0.53	0.29-0.59
Diego Garcia	0.22-0.52	0.25-0.55	0.34-0.66
Gan	0.22-0.49	0.26-0.53	0.33-0.63
Colombo	0.21-0.48	0.25-0.53	0.32-0.62
Sabang	0.19-0.50	0.26-0.54	0.31-0.60
Zanzibar	0.23-0.52	0.26-0.54	0.35-0.64
Sibolga	0.17-0.49	0.24-0.53	0.28-0.60
Hanimadhoo	0.22-0.48	0.26-0.53	0.33-0.63
Male	0.22-0.48	0.26-0.53	0.33-0.63
Minicoy	0.21-0.48	0.26-0.53	0.32-0.62

2081-2100	RCP2.6	RCP4.5	RCP8.5
Point La Rue	0.26-0.69	0.32-0.74	0.48-0.99
Padang	0.21-0.64	0.31-0.73	0.41-0.9
Diego Garcia	0.26-0.68	0.33-0.75	0.48-1.0
Gan	0.27-0.64	0.34-0.73	0.47-0.96
Colombo	0.25-0.62	0.33-0.72	0.46-0.94
Sabang	0.23-0.65	0.33-0.74	0.44-0.92
Zanzibar	0.28-0.68	0.34-0.75	0.50-0.98
Sibolga	0.21-0.64	0.31-0.74	0.41-0.92
Hanimadhoo	0.26-0.63	0.34-0.73	0.47-0.96
Male	0.27-0.63	0.34-0.73	0.47-0.96
Minicoy	0.26-0.62	0.33-0.73	0.46-0.95

Table 3.5: *Projected ranges of sea level rise for equatorial Indian Ocean locations over the period 2061-2080 (left) and 2081-2100 under RCP2.6, RCP4.5 and RCP8.5 relative to a baseline period of 1986-2005.*

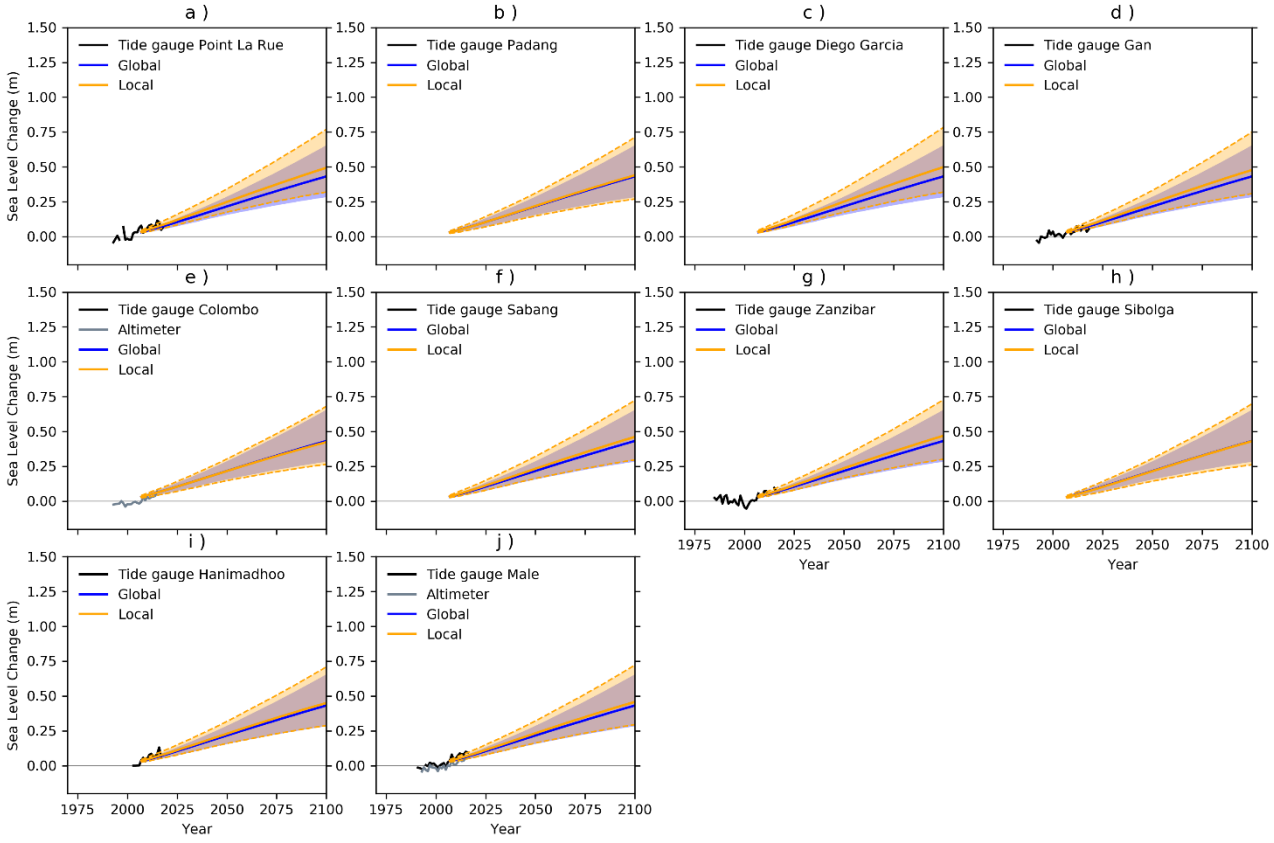

Figure 3.7: *21st century sea level projections for RCP2.6 at tide gauge locations in the Equatorial Indian Ocean based and projected GMSL changes. Solid lines indicate the central estimate, shaded areas indicate the 5th - 95th percentile range for projected local (yellow) and global (blue) changes.*

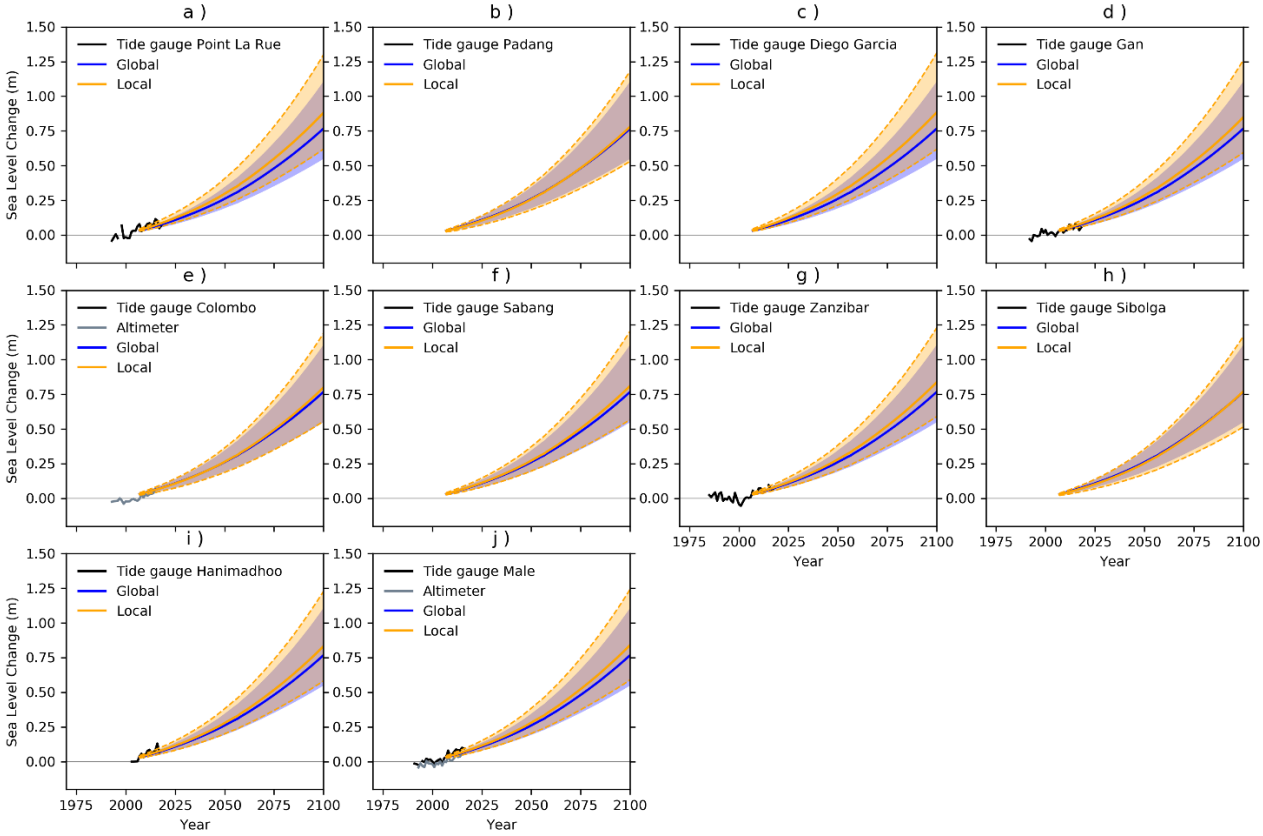

Figure 3.8: *21st century sea level projections for RCP8.5 at tide gauge locations in the Equatorial Indian Ocean based and projected GMSL changes. Solid lines indicate the central estimate, shaded areas indicate the 5th - 95th percentile range for projected local (yellow) and global (blue) changes.*

3.4 Exploring the drivers of coastal sea level change

In this section we explore geographical variations in 21st century sea level changes and examine the relative contribution to sea level changes from different physical processes, using projections from selected locations from the Arabian Sea and the Bay and Bengal. We also discuss the role of different drivers of coastal sea level change, including natural variability, climate change forcing scenarios, and modelling uncertainty (following Hawkins & Sutton, 2009).

Karachi (Pakistan) and Cochin (India) are used to illustrate the range of sea level projections for the Arabian Sea. The total range of projected sea level rise at 2100 across the three RCP scenarios is approximately 0.11-0.82 m for Karachi and 0.24-0.92 m for Cochin. At both Karachi and Cochin, the leading contribution to total sea level rise is from changes to ocean circulation and density represented by the sterodynamic component. For example, at Karachi and Cochin the sterodynamic component accounts for approximately 45-60 % and 45-55% of the total change at each location respectively (figure 3.9). However, the differences in projected changes

between Karachi and Cochin are largely determined by the (scenario independent) land water storage component (purple lines in figure 3.9) and the spatial pattern of change from land water storage change (figure 3.11) from GRD. The difference between projected changes at Cochin and Karachi for 2081-2100 is around 0.11 m-0.12 m across the three RCPs. The scenario independent land water component for Karachi ranges from -0.18 m to 0.02 m but for Cochin contributes between zero and 0.01 m. The difference in the central estimate for land water components at Karachi and Cochin (-0.08 m) represents 70-75% and of the difference in central estimates for projected changes at the two sites across the three RCPs.

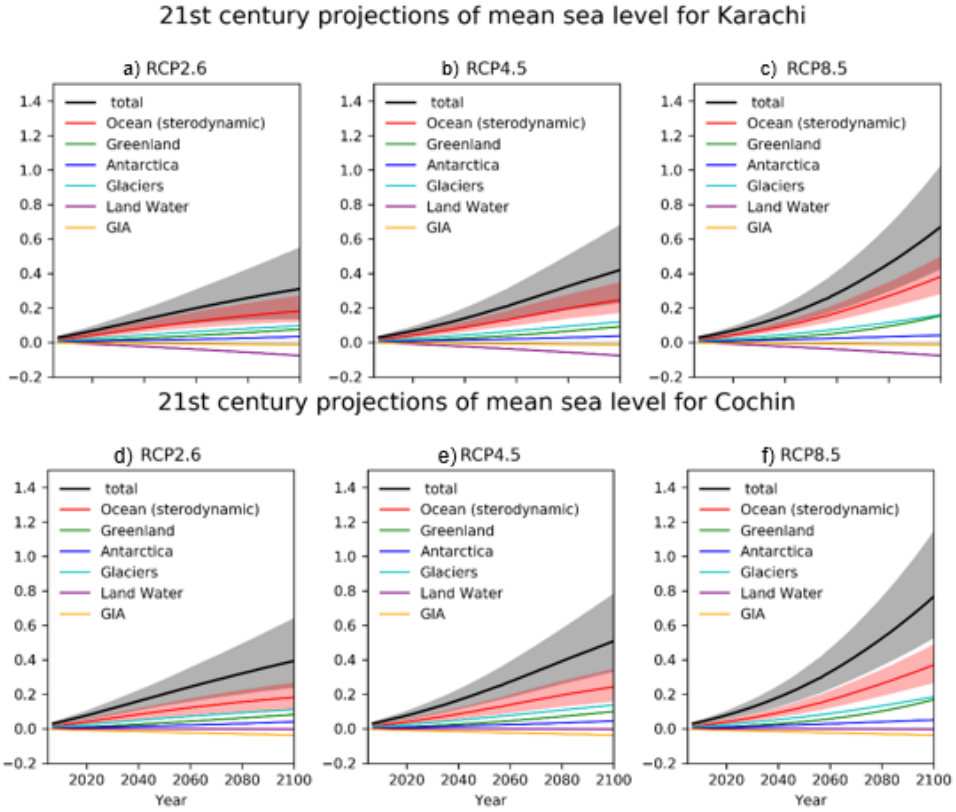

Figure 3.9: *Sea level projections for two locations on the Arabian Sea, showing contributions to sea level change from individual components. All timeseries are plotted relative to a baseline period of 1986-2005. Coloured lines indicate the central estimate according to the figure legend. Shaded regions present the projection range for the sea level component (right panels) under the RCP scenario indicated by the panel titles.*

Chittagong (Bangladesh) and Port Blair (Andaman and Nicobar Islands, Indian union Territory) are used to illustrate the range of sea level projections for the Bay of Bengal (figure 3.7). Across the three scenarios, the total range for projected sea level changes over 2081-2100 relative 1986-2005 is 017– 0.86 m at Chittagong and 0.24 –0.92 m at Port Blair. As with the Arabian Sea, the sterodynamic component of sea level change represents the largest individual component but also contributes to some of the

difference between sites. The difference between total changes at Port Blair and Chittagong is within 0.05-0.06 m for the three RCPs. Differences for the sterodynamic components account are -0.01 m -0.03 m for RCP2.6, -0.01 m – 0.01m for RCP4.5 and less than a centimetre for RCP8.5, while for the glacier component the difference are 0.01-0.02 m for RCP2.6 and RCP4.5, rising to 0.01-0.03 for RCP8.5, the same order as the difference for the land water component 0.00-0.03 m. Hence there is no clear dominant sources of differences in projected sea level rise at the two sites.

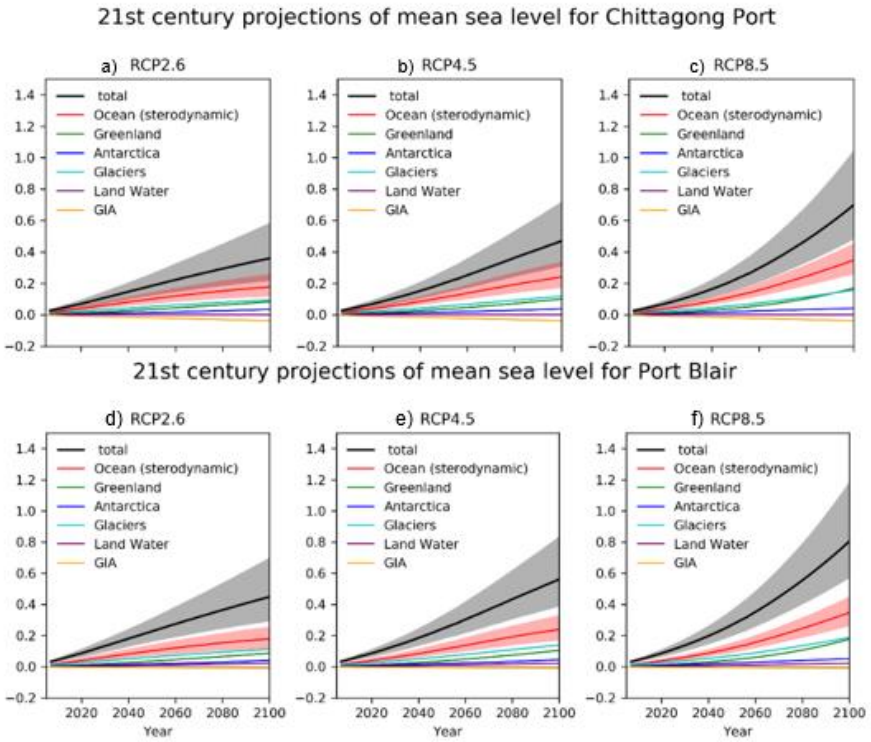

Figure 3.10: *Regional sea level projections for two locations on the Bay of Bengal, showing the contributions to sea level change from individual components. All timeseries are plotted relative to a baseline period of 1986-2005. Coloured lines indicate the central estimate according to the figure legend. Shaded regions present the projection range for the corresponding RCP scenario (left panels) or sea level component (right panels).*

Note that the land water storage estimates used in this study assumes that 100% of the abstracted groundwater ends up in the oceans, however more recent estimates suggest fraction reaching the oceans is approximately 80% (Wada et al. 2016). Due to the spatial patterns of sea level change from the loss of terrestrial water mass through ground water extraction (figure 3.11), the inclusion of the updated land water storage estimate would increase total sea level changes in areas where the land water component is negative (blue shaded areas in figure 3.11), because of the reduced negative contribution but increase sea level elsewhere. Although the land water storage component is scenario independent, the influence of this contribution on total

sea level diminishes relative to components that do increase for higher RCPs (e.g. for South Asia the sterodynamic, glacier and Greenland ice sheet terms in figure 3.10). Therefore, the updated land water storage estimate would be most evident for RCP2.6 at areas in the north Arabian Sea and northwest Bay of Bengal where the spatial gradient in land water contribution are strongest and the contribution changes sign (see figure 3.11).

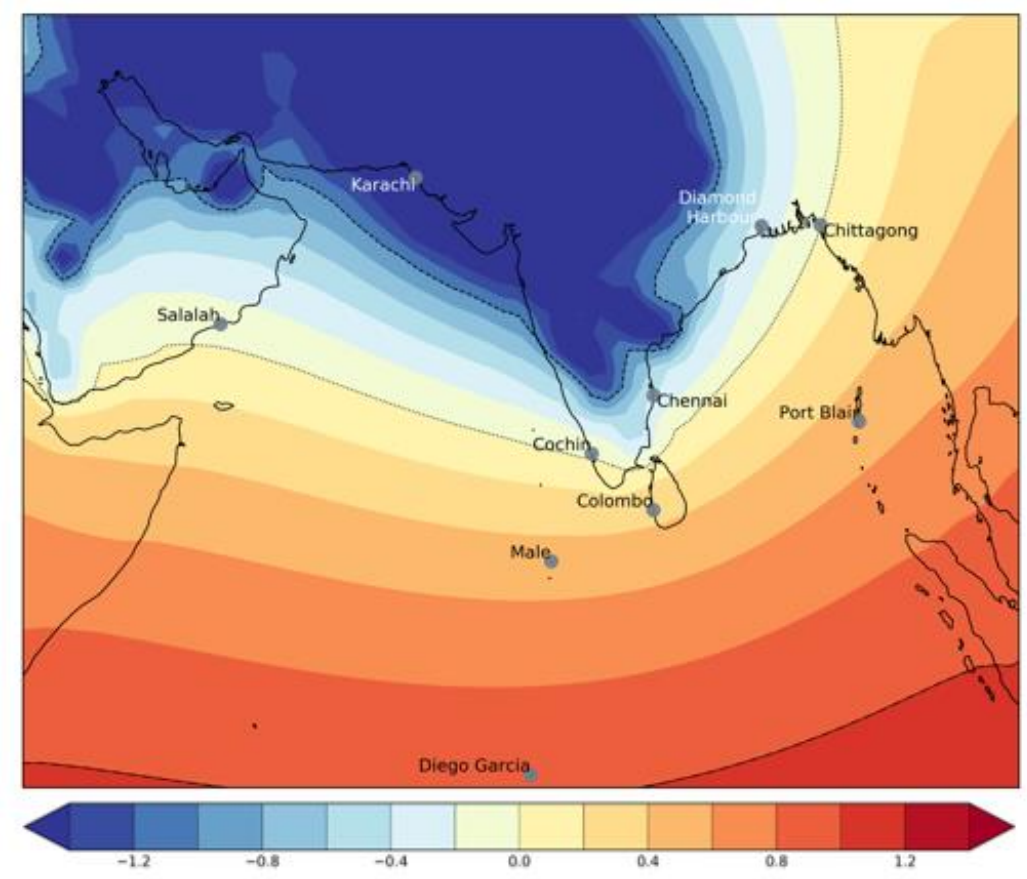

Figure 3.11: *Gravitation-Rotation-Deformation (GRD) pattern for mean sea level changes due to changes in land water storage, expressed as the changes in in local sea level per unit rise in land water component of GMSL. The zero contour is indicated by the dotted line. The positive and negative unit contours are indicated by the dashed lines. Sample locations are shown (grey circles) to indicate the variations in contributions from land-based water mass changes. Note the negative contributions at Karachi, Salalah, Chennai and Diamond Harbour, the near zero contributions at Chittagong and Cochin.*

Recall, that land water storage (also referred to as terrestrial water storage) refers to the liquid water mass stored on land in natural and artificial reservoirs. Human activities such as groundwater extraction, that remove water mass from terrestrial water stores, can contribute to global sea level rise by transferring fraction water mass from the land to the world's oceans. In contrast human activities that increase the amount of water mass that can be stored on land, such the construction of artificial reservoirs or dams

(hereafter referred to as dam impoundment), reduce the fraction of water transferred from land to the oceans by the hydrological cycle and can reduce the rate of global mean sea level rise.

The projections for changes in land water storage used in this study are based on statistical relationships between historical changes in groundwater extraction and water impoundment*. Groundwater extraction is projected to increase as both population growth and enhanced evaporation loss are expected increase water demand. Dam impoundment has tended to decline with population growth, resulting in a net positive contribution to global sea level rise from land water storage over the late 20th century and this projected to increase over the 21st century. As with contributions to global sea level rise from terrestrial ice mass loss (e.g. ice sheets and glaciers), the effects of terrestrial water mass loss on local sea level are characterised by near-field fall in sea level around locations of water mass loss and far-field increase in sea level elsewhere. Figure 3.11 shows the near-field negative contribution to sea level from land water storage over the South Asian landmass, from projected increases groundwater extraction over the region. It should be noted that the projections do not include vertical land movement processes other than those associated with GRD and do not account for land subsidence, which often results from groundwater extraction. Hence the negative contribution of land water through GRD does not contradict previous studies that indicate that groundwater extraction is often associated with increased rates of relative sea level rise (e.g. at Manilla in the Philippines, Kahana et al., 2016)[5] due to land subsidence (i.e. reductions in the elevation of tide gauge stations relative to the sea floor).

Tide gauge locations from the two basins, show substantial year-to -year variability in the annual mean sea level based on the PSMSL tide gauge records. The variability can be quantified by calculating the standard deviation in annual mean sea level from the tide gauge records on PSMSL. For example, the variability Karachi and Cochin have typical ranges of +/- 0.096 m and +/- 0.052 m. While for Chennai and Cox's Bazaar the ranges are +/- 0.052 m and +/- 0.184 m respectively. It is important to note that this sea level variability will be superimposed on the long-term projected sea level rise. While ranges are small compared to the sea level rise at the locations for 2100,

[5] *From pervious DFID-funded Met Office work*
http://www.precisrcm.com/DFID_Philippines_Reporting/Philippines_Sea_Level_Report_Oct_2016.pdf

the variability is an important consideration on shorter timescales (e.g. over the next two decades, and particularly for the lower emission scenarios). For the first half of the 21st century, the projected sea level changes for the different RCP scenarios are broadly similar but differences emerge during the late the 21st century and these differences become more significant over the extended period (section 4.3). Following Hawkins and Sutton (2009), the increasing importance of the RCPs scenario can be seen in the increasing contribution to overall uncertainty (standard deviation) in sea level change (figure 3.13) at different tide gauge locations. Tide gauge records were used to estimate the coastal sea level variability at each location using records from PSMSL. These are combined with an estimate of the uncertainty arising from the different RCP scenarios and the modelling uncertainty (i.e. the average 5th to 95th percentile range of sea level rise across the RCPs) to give a first order picture of the importance of the factors over the 21st century (figure 3.12).

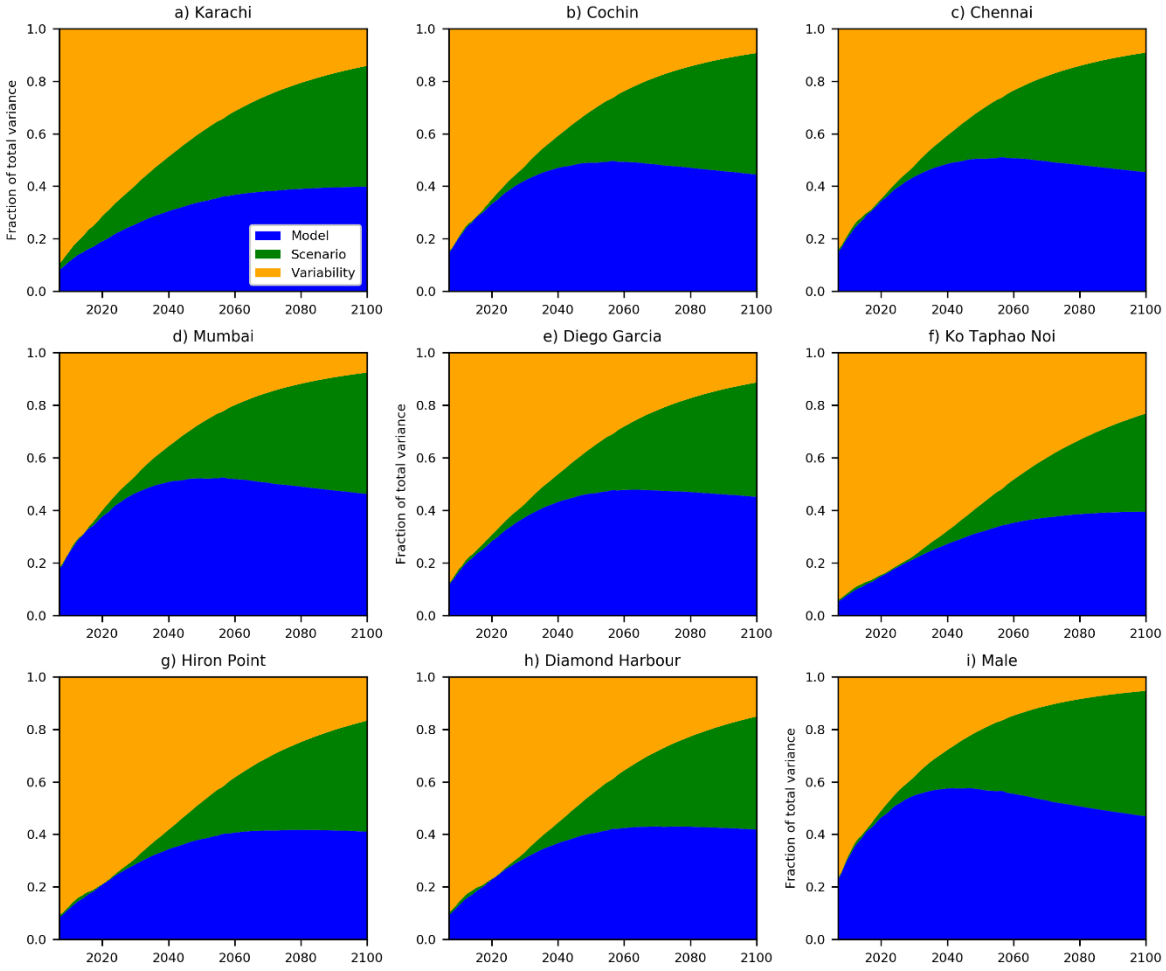

Figure 3.12: *The fraction of sea level rise uncertainty at selected South Asia tide gauge locations from: sea level variability (yellow); climate change scenario (green); and model uncertainty (blue), following Hawkins and Sutton (2011) based on annual mean data.*

Also shown in figure 3.12 is the increasing importance of differences between the underlying climate models to overall uncertainty in sea level change over 21st century. For stakeholders interested in relatively short time horizons, e.g. 2020s to 2040s, coastal variability will be an important consideration. The best information publicly available information on observed sea level variability in the South Asia comes from the network of tide gauges supplying data to PSMSL, although many of the tide gauge records contains large gaps and few stations have long-duration sea level records (>30yrs). Not all tide gauge instruments for a given country are available on PSMSL and datasets based on additional tide gauge stations have appear in the literature. For Bangladesh and Indian West Bengal (Becker et al., 2020) presented spatially averaged water level data, based on a large sample of water level records and found the variability seen in the PSMSL records from Bangladesh are broadly consistent with larger sections of coastline.

4. Exploratory extended projections of sea level changes to 2300

Section summary

In this section we briefly discuss the exploratory GMSL projections (section 4.1) for extended the period 2100-2300 presented in Palmer et al (2020). We then present exploratory regional coastal projections (section 4.2) of time mean sea level for the extended period 2100-2300. There is inherently more uncertainty associated with generating information for the extended range period than for the 21st century. The results should be taken as illustrative of the potential future changes and we have a lower degree of confidence in the absolute values reported. For these extended time-horizons there is a marked divergence between RCP8.5 and the two other climate change scenarios used in this study. RCP2.6 is the only scenario to show a decrease in CO^2 concentrations and global mean surface temperature (GMST) in the coming centuries. RCP4.5 is characterised by a slow increase in GMST after 2100 as atmospheric concentrations of CO2 stabilizes. Under RCP8.5, the CO2 concentration continues to rise rapidly after 2100 before a smooth transition to stable CO2 concentrations after 2250 (see figure 4.1)

For Karachi, Pakistan the projection ranges at 2300 are approximately 0.2-1.8m, 0.7-4.3 m for RCP2.6 and RCP8.5 respectively. For Male, Maldives the projection range are 0.6-2.1 m and 1.3-4.7 m for RCP2.6 and RCP8.5 respectively. In the Bay of Bengal, the projected ranges for Chittagong in Bangladesh are 0.6 -1.7 m and 1.1 – 4.3 m for RCP2.6 and RCP8.5. For Port Blair in Andaman and Nicobar Island, Indian union territory the projected ranges are larger for the high emission scenarios, with 0.6-2.1 m and 1.3-4.6 m for RCP2.6 and RCP8.5 respectively.

4.1 Climate forcing and surface temperature response

The extended projections presented here use the representative concentration pathway (RCP) scenarios and their corresponding extended concentration (ECP) pathways, as described by Meinshausen et al. (2011). The ECPs are simple extensions to the RCP beyond 2100 based on the assumption of either smoothly stabilizing concentrations or constant emissions (figure 4.1). The strong mitigation scenario RCP2.6 has constant negative CO2 emission after 2100 (figure 4.1 left panel, dark blue line), leading to atmospheric concentration for CO2 falling to 360 ppm by 2300. For RCP4.5 (figure 4.1 left panel, light blue), CO2 concentration undergo a smooth transition to constant values after 2150 by linear adjustment of emission from 2100. The same procedure is followed for RCP8.5 but the stabilization of CO2 concentrations delayed until 2250 (figure 4.1 left panel, red), with linear adjustment from 2150 emissions. The scenario extensions can be considered as sensitivity studies and should not be interpreted as showing the full range of post 2100 behaviour, or even the most likely behaviour.

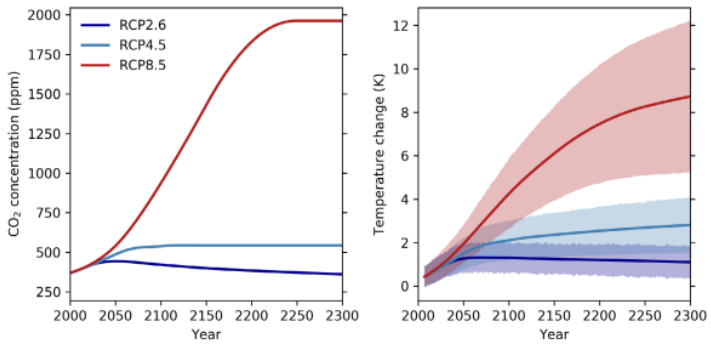

Figure 4.1: *From UKCP18 Marine (Palmer et al. 2018a). (left) Extended carbon dioxide concentration under RCP2.6, RCP4.5 and RCP8.5. (right) The associated global mean surface temperature (GMST) change for the Two-Layer model ensemble used in the extended sea level projections (see methods section). Temperature change is shown relative to a 1986-2005 baseline. Shaded regions represent the projection range for the corresponding RCP scenario.*

The global surface temperature response associated with the extended RCPs is evaluated using the same two-layer simulations that form the basis of the extended sea level projections. At this extended timescale, the RCP8.5 scenario results in much larger C02 concentrations than the other two scenarios and a correspondingly large global mean surface temperature (GMST) response (figure 4.1 right panel, red). The larger temperature response is associated with very large uncertainties, as seen in the 5th to 95th range of temperatures changes (figure 4.1, right panel red shaded area) and reflects the range of climate sensitivities among CMIP5 climate models (Andrews et al., 2012; Knutti & Hegerl, 2008). We note that these levels of surface temperature rise take climate models beyond the regime in which they were validated against observations, and therefore the 2100-2300 sea level projections should be treated with caution.

Despite the stabilisation of CO2 concentrations in RCP4.5 from 2150, the GMST continues to rise over the coming centuries. The delayed response to CO2 stabilisation is a well-known feature of the climate system and associated with the slow response of the global ocean to the imposed climate forcing (Collins et al., 2013; Knutti & Hegerl, 2008; Nicholls & Lowe, 2004). RCP2.6 is the only scenario to show a decrease in GMST, with temperatures reaching a peak in the 21st century. Note the emulated model simulations used in the extended time mean sea level projections tend to slightly underestimate the reduction in GMST at 2300 compared to the few CMIP5 models simulations that do provide data for the extended period 2100-2300 (Matthew D Palmer et al., 2018b)

The central estimate for surface temperature changes at 2300 (based on the Two-Layer model simulations, described in methods section) are approximately 1.3C, 2.4C and 8.C for RCP2.6, RCP4.5 and RCP8.5 respectively relative to baseline period of 1986-2005.

4.2 Global extended range sea level projections

The extended global time mean sea projections are identical to those presented in Palmer et al (2020) based on methods used for UKCP18 (Lowe et al., 2018) and discussed in (Palmer et al., 2018a) and (Palmer et al., 2018 b). As with the 21st century sea level projections, the extended projections are based on model simulations of global surface temperature and global thermosteric sea level (global thermal

expansion). However, since most of the CMIP5 models used in 21st century projections do not provide data on the relevant variables[6] out to 2300, we use a physically based emulator to generate a set of emulated CMIP5 models that have been tuned to mimic the characteristics of the original GCMs over the 21st century and extended the simulation out to 2300. See the supplementary material and methods document for details.

The advantage of these methods is that it provides a set of extended projections that can be used alongside the 21st century sea level projections, since these are based on the same underlying CMIP5 models and produce a similar range of values over the 21st century. The extended projections are directly traceable to CMIP5 climate model simulations and methods of IPCC AR5 (Church et al. 2013).

The extended projections show that GMSL continues to rise over the coming centuries under all scenarios. The continued rise in sea level seen in the extended sea level projections demonstrates the long-term commitment to sea level rise, associated with anthropogenic forcing of the climate system and the long timescale response of the ocean and process of land-based ice loss. The directly driven climate responses are compounded by the expectation of future groundwater extraction in order to maintain water available (e.g. Wada et al. 2012; Church, 2013). Even under RCP2.6, the most aggressive mitigation scenario the central estimate of GMSL sea level rise exceeds 1m by 2300. The central estimates are 1.5 m for RCP4.5 and 2.5 m for RCP8.5.

For the extended period, the contribution to sea-level rise from the different physical processes varies with the climate scenario. Under RCP4.5, the contribution from thermal expansion, Greenland ice loss and glacier ice loss represent the dominant contributions to the mid-point estimate for GMSL rise for much of period. During the 23rd century, the total remaining glacier mass is depleted, and ceases to contribute to further GMSL rise. For RCP8.5, the remaining glacier mass become depleted around 2150 in the central estimate, with thermal expansion and Greenland ice mass loss making the dominant contribution to GMSL rise over the remainder of the period. The central estimate for the contribution to GMSL rise from Antarctica ice mass loss lower for RCP8.5 is dominated by the surface mass balance component and enhanced snow accumulation leads to a lower contribution than under RCP4.5. The large uncertainty

[6] CMIP5 variables for global mean surface temperature (*'tas'*), global thermal expansion (*'zostoga'*)

in the GMSL rise under RCP8.5 is dominated by uncertainties in magnitude of ice loss from dynamic ice discharge.

The projections for GMSL rise to 2300 are associated with much large uncertainties than the projections over the 21st century and there is lower confidence that the uncertainties span the range potential outcomes. For 2300 the uncertainties (table 4.1) span the range 0.5 m-1.0 m for RCP2.6 and RCP4.5, with 1.5-2.0 m for RCP8.5. In all case the uncertainties are non-symmetric, with greater uncertainty for higher values in timeseries for the components of sea-level rise and total sea level rise (figure 4.2).

		Sea level change (m)		
	Year	**RCP2.6**	**RCP4.5**	**RCP8.5**
21st century projections	**2100**	0.28-0.65	0.37-0.78	0.55-0.98
Exploratory extended-range projections	**2100**	0.28-0.59	0.35-0.70	0.51-0.98
	2200	0.4-1.3	0.7-1.7	1.3 – 2.9
	2300	0.5-1.9	0.9-2.4	1.7 – 4.4

***Table 4.1**: Comparison of the 21st sea level projections (section 3) and the extended projections presented in this section. Numbers beyond 2100 quoted to the nearest 0.1 m, due to the lower confidence associated with projections over the extended period.*

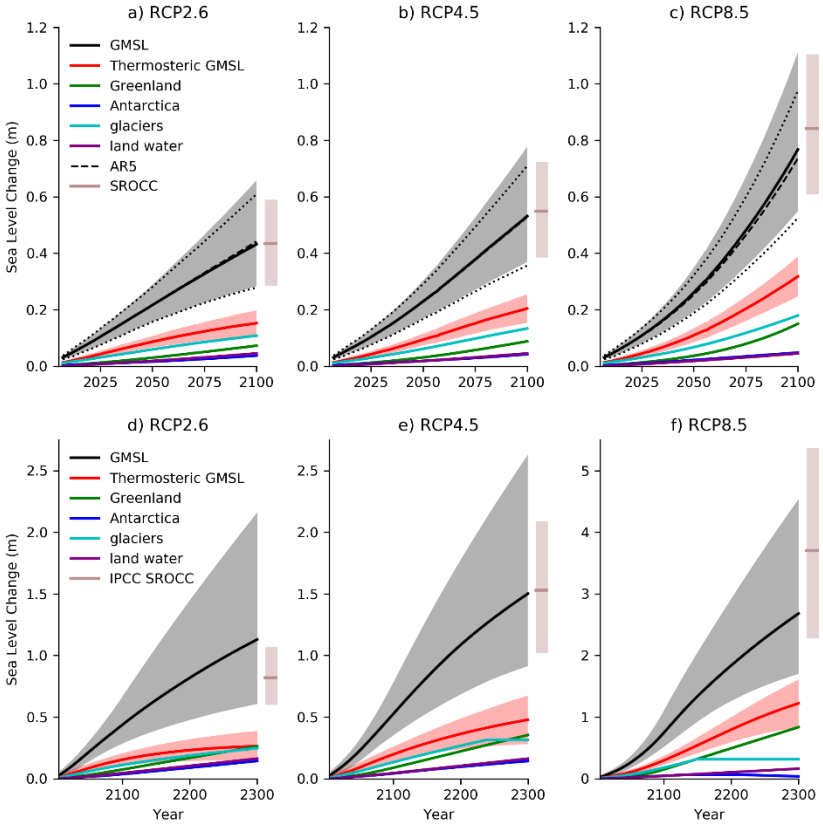

Figure 4.2: *Projections of global time-mean sea level change for 21st century (top row) and extended projections to 2300 (bottom row) both relative to a baseline period of 1986-2005. The different sea level components are indicated by the coloured lines. The projection ranges are indicated by the shaded regions for the total sea level rise and thermosteric sea level rise (sea level rise due to global thermal expansion).*

4.3 South Asia extended range sea level projections

As with the 21st century South Asia regional sea level projections (section 3.2), the exploratory extended range regional projections are derived from global time-mean sea level projections for the period 2100-2300. The regional extended range projections span a wider range than the extended GMSL projections, reflection the greater uncertainty associated with sea level changes at the regional scale, particularly for the higher RCPs. The extended local sea level projections generally follow the time evolution of global sea level projections (figure 4.2). The projected changes for locations in the Arabian Sea and Bay of Bengal regions are generally lower than at locations in the equatorial Indian Ocean.

Arabian Sea:

The projected sea level changes under RCP2.6 for the Arabian Sea (figure 4.3a) over the extended period are smaller than the projected GMSL changes for RCP2.6. The

largest projected changes continue to be found at southern locations (e.g. Cochin panel figure 4.3a), with lowest projected changes in the northeast of the region (e.g. Karachi panel figure 4.3a). In the north of the Arabian sea there is a weak zonal gradient in projected changes, with slightly larger projected changes at Chabahar (Iran) compared to Karachi (Pakistan). Under RCP8.5, the likely range (as indicated by the yellow shaded regions in figure 4.4a) is spans a wider range than likely range for GMSL changes (blue shaded area). At all locations the central estimates for projected changes are larger than the central estimate for global changes for much of the extended period.

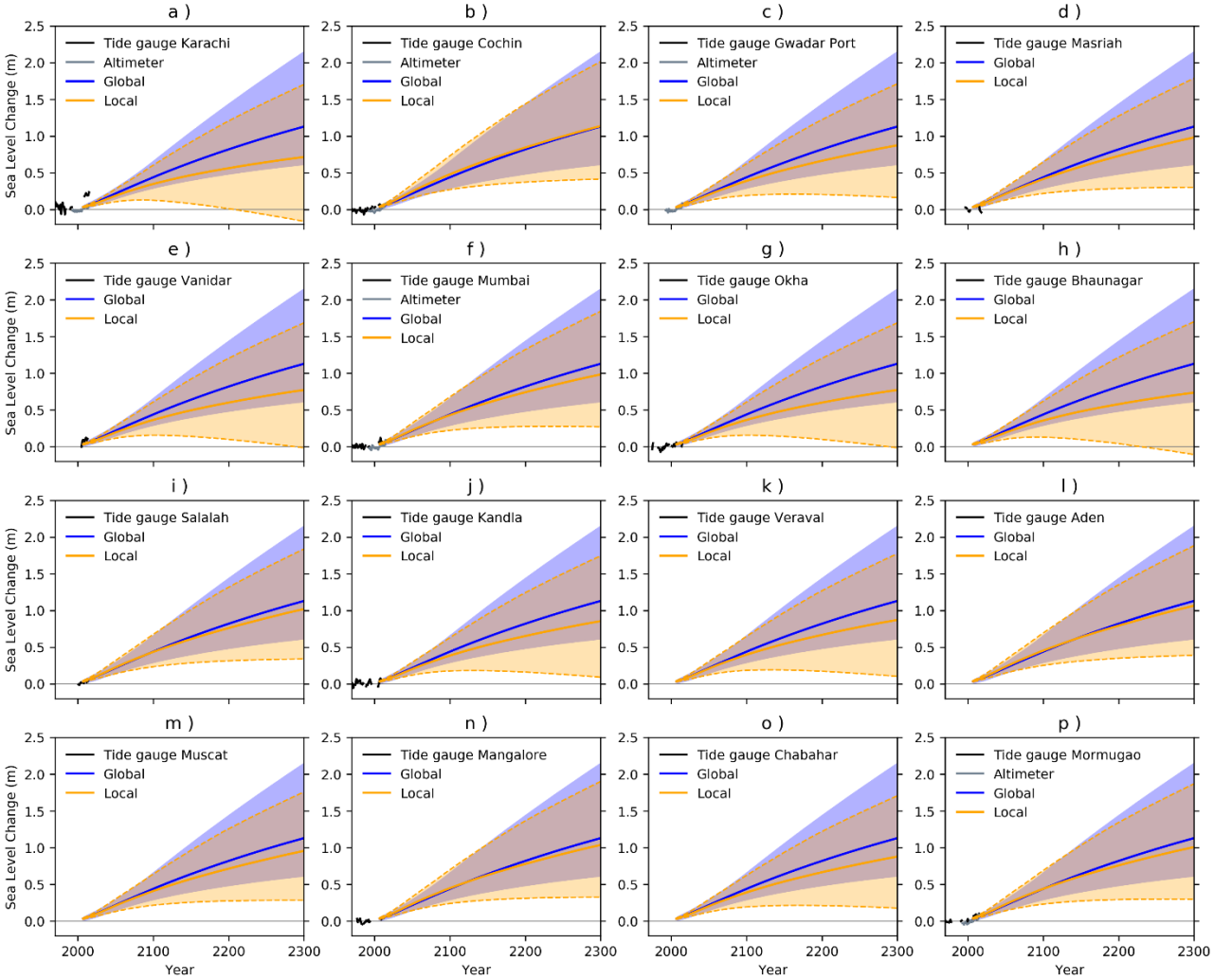

Figure 4.3: *Extended range projections under RCP2.6 of local sea level for the Arabian Sea, based on the nearest tide gauge location compared with the corresponding GMSL timeseries. The solid lines indicate the central estimate and the shaded areas indicate the 5th to 95th percentile range, yellow for the location changes and blue for global changes.*

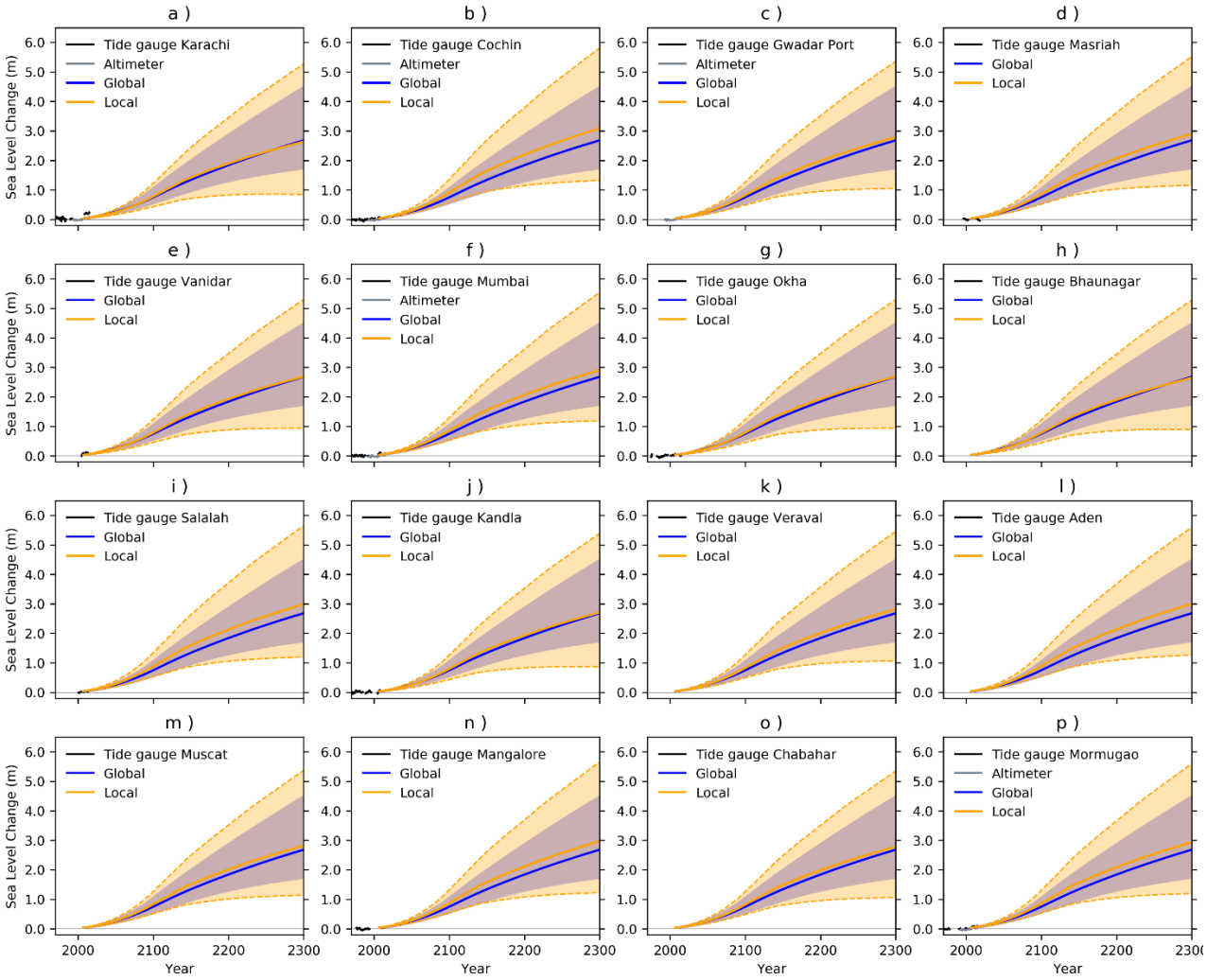

Figure 4.4: *Extended range projections under RCP8.5 of local sea level for the Arabian Sea, based on the nearest tide gauge location compared with the corresponding GMSL timeseries. The solid lines indicate the central estimate and the shaded areas indicate the 5th to 95th percentile range, yellow for the location changes and blue for global changes.*

Bay of Bengal:

For the Bay of Bengal, the projected under RCP2.6 over the extended period demonstrate similar patterns to those seen in the 21st century projections, with larger changes in the south(Port Blair panel figure 3.4b) relative to the north (Chittagong panel figure 4.3b) and larger changes in the east relative to the west for a given latitude (e.g. between panels for Port Blair and Nagapattinam).

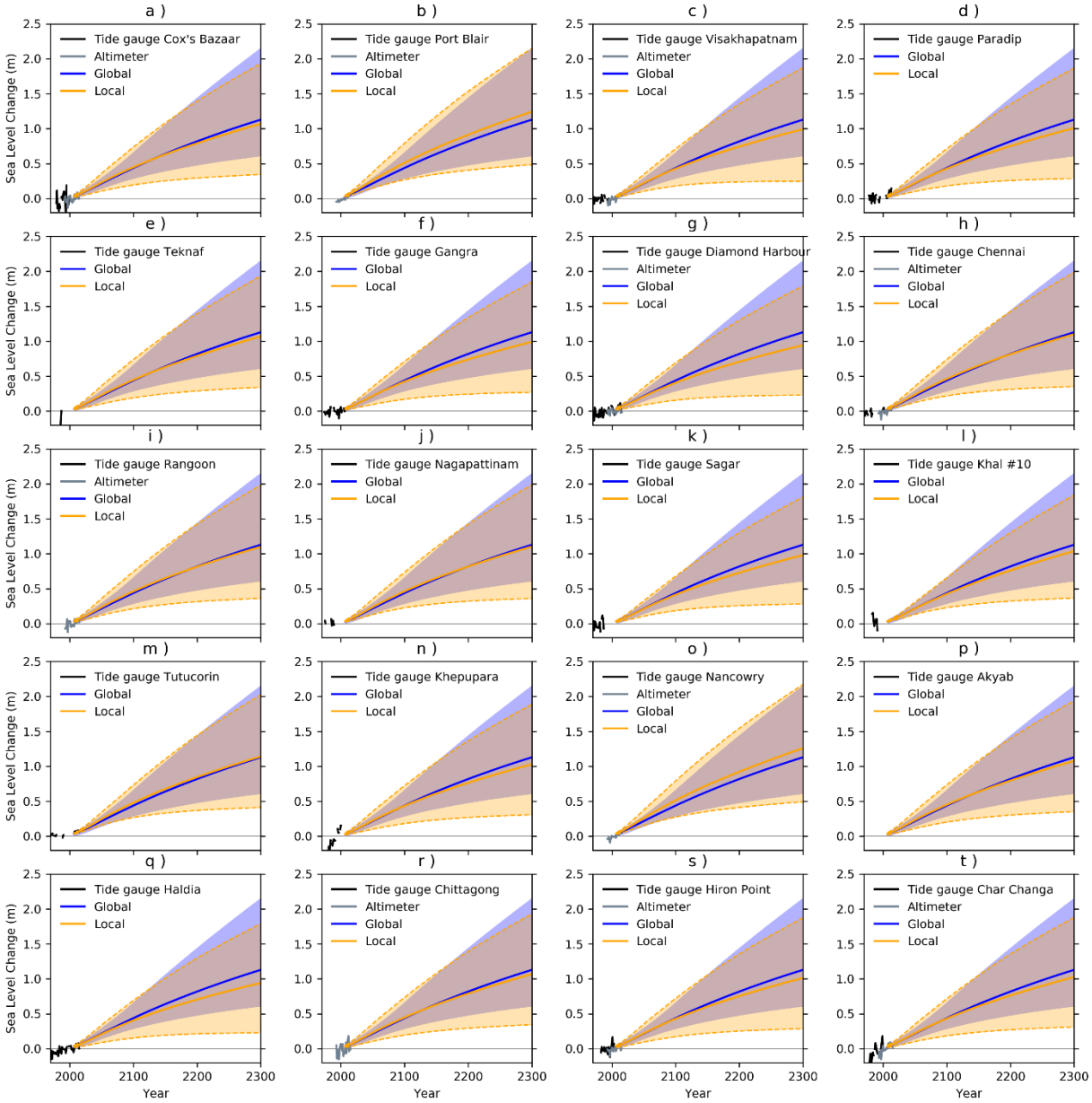

Figure 4.5: *Extended range projections under RCP2.6 of local sea level for the Bay of Bengal, based on the nearest tide gauge location compared with the corresponding GMSL timeseries. The solid lines indicate the central estimate and the shaded areas indicate the 5th to 95th percentile range, yellow for the location changes and blue for global changes.*

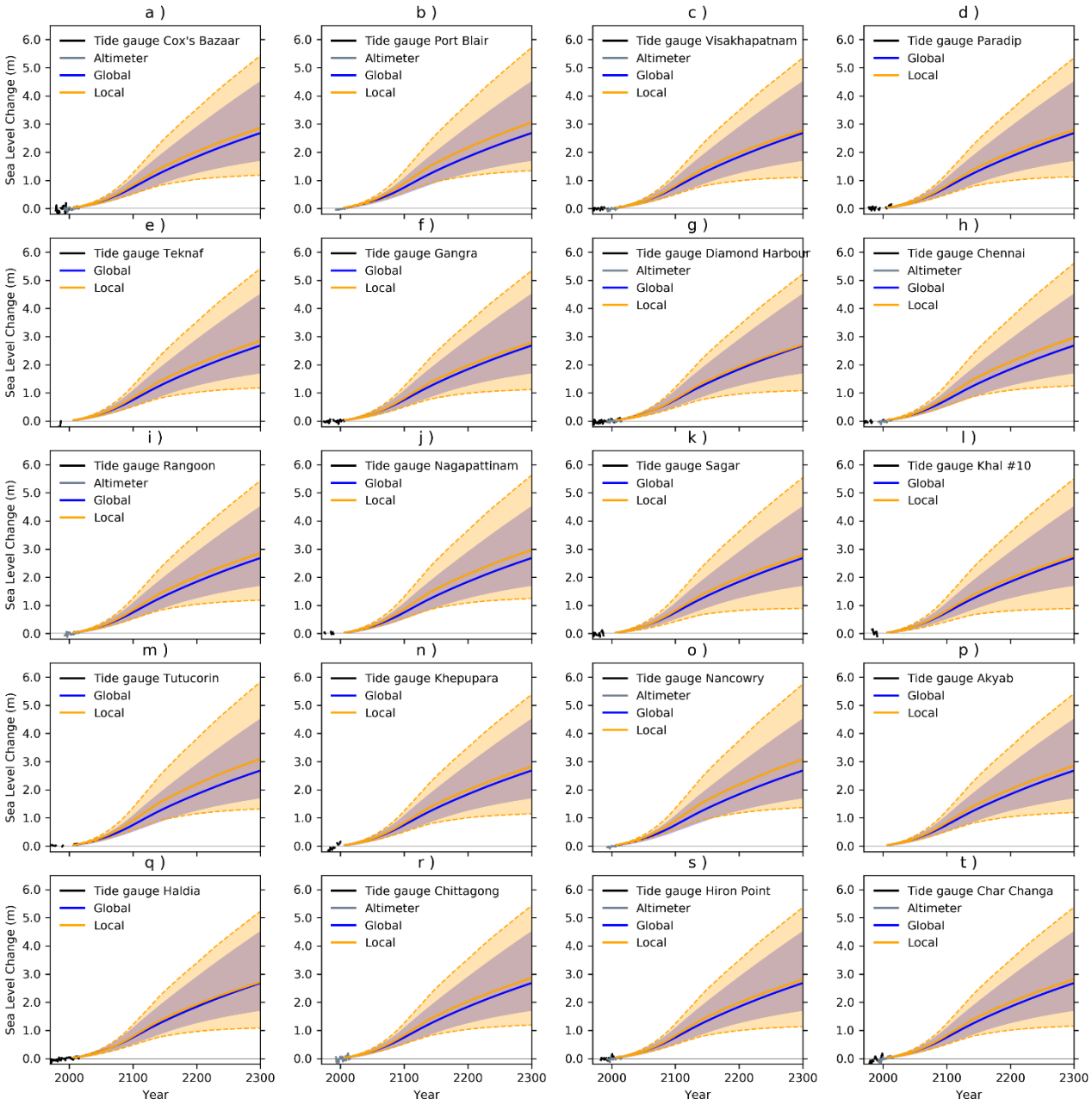

Figure 4.6: *Extended range projections under RCP8.5 of local sea level for the Bay of Bengal, based on the nearest tide gauge location compared with the corresponding GMSL timeseries. The solid lines indicate the central estimate and the shaded areas indicate the 5th to 95th percentile range, yellow for the location changes and blue for global changes*.

Equatorial Indian Ocean:

Of the cities in the region, Male in the Maldives and Columbo in Sri-Lanka show the largest values for sea level rise. The projected ranges under RCP2.6, RCP4.5, and RCP8.5 for Male are 0.5-2.0 m, 0.8-3.0 m, and 1.3-6.0 m, while for Columbo these are 0.4-2.0 m, 0.7-3.0 m, and 1.2-5.8 m. The broader spatial patterns over the region are expected to be qualitatively robust but the actual values for sea level change over the extended period should be treated with lower confidence.

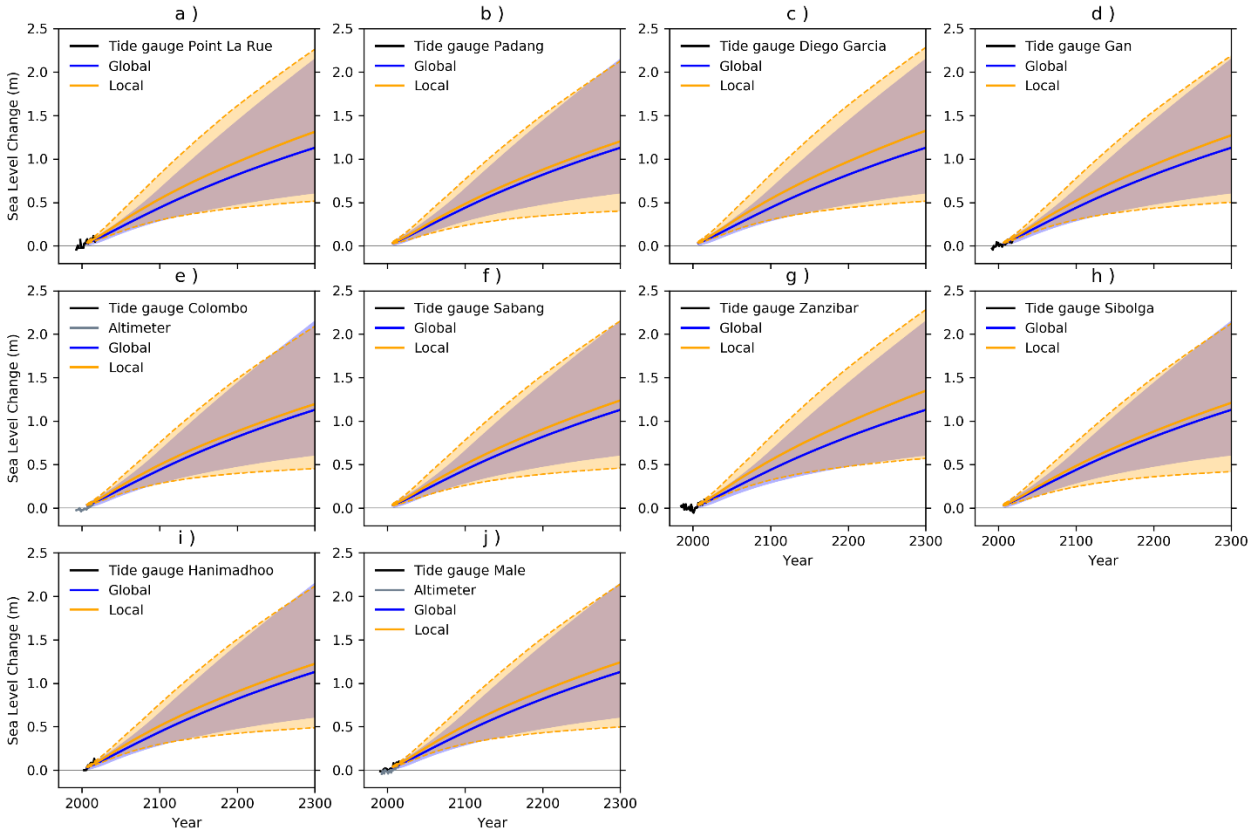

Figure 4.7: *Extended range projections under RCP2.6 of local sea level for the Equatorial Indian Ocean, based on the nearest tide gauge location compared with the corresponding GMSL timeseries. The solid lines indicate the central estimate and the shaded areas indicate the 5th to 95th percentile range, yellow for the location changes and blue for global changes*

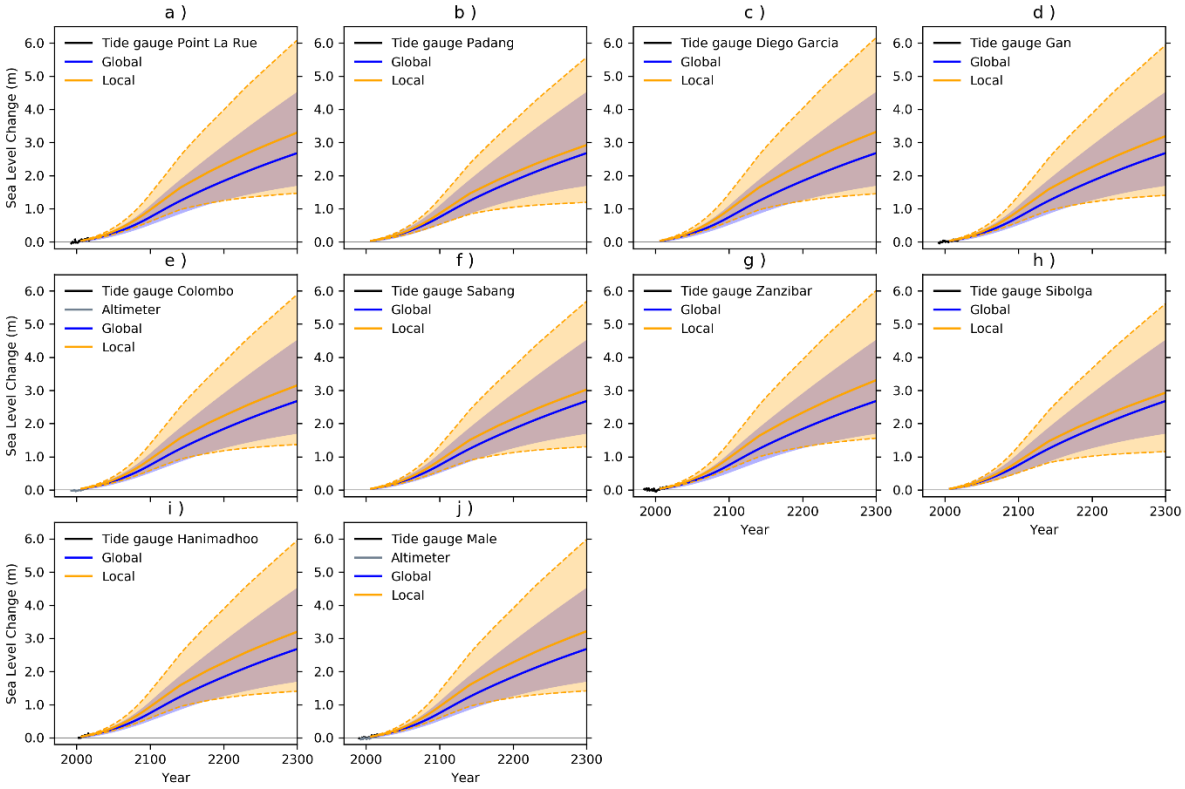

Figure 4.8: *Extended range projections under RCP8.5 of local sea level for the Equatorial Indian Ocean, based on the nearest tide gauge location compared with the corresponding GMSL timeseries. The solid lines indicate the central estimate and the shaded areas indicate the 5th to 95th percentile range, yellow for the location changes and blue for global changes*

4.4 Long-term drivers of regional sea level change

Under RCP4.5 and RCP8.5, the sterodynamic component (i.e. local ocean thermal expansion and circulation change) is dominant driver of sea level rise, which is slightly offset by the negative (and scenario independent) contributions from glacial isostatic adjustment (GIA) and land water storage. Under the aggressive mitigation scenario RCP2.6, there are locations where the range of projected changes includes, the potential for a net fall in sea-level by 2300 (e.g. Karachi panels figures 4.3 and 4,4, top left). For locations on the Pakistan coastline, the combination of GIA and land water storage, offset the lower bound sterodynamic contribution. For all scenarios, we see a deceleration of sea level rise after the 21st century. However, we cannot rule out the possibility of increases to the rate of sea level rise beyond the 21st century due to collapse of the west Antarctic ice sheet.

5. Next steps

In this section we briefly discuss future work needed to build on the South Asia sea level projections presented in this study. Some areas are part of ongoing work within the CARISSA project.

The study has not provided information on future changes to coastal sea level extremes. While we acknowledge the importance of information on coastal sea level extremes in coastal impacts assessment and risks management, we expect that changes in coastal extremes over the coming decades and centuries will be largely determined by changes in mean sea level (Church et al., 2013). Small changes in mean sea level can result in significant changes in the return periods for extreme coastal water levels (Oppenheimer & Glavovic, 2019). A full treatment of this subject for South Asia will require high frequency timeseries for water levels at a given location and collaboration with stakeholders to identify the relevant return periods, exceedance thresholds and allowances (Howard & Palmer, 2020), combined with an understanding of planning time-horizons and user uncertainty tolerance (Le Cozannet et al., 2017; Hinkel et al., 2019; Kopp et al., 2019).

Additional contributions to changes in coastal sea level extremes could arise from changes to tropical storm characteristics on surge/wave heights, for example storm frequency, intensity and their trajectories (Jisan et al., 2018; Rahman et al., 2019; Woodruff et al., 2013). At present however, there is low confidence in projected changes to storm characteristics at basin and sub-basin scale (Knutson et al., 2012; Walsh et al., 2012). While the majority of tropical storm related deaths have been in the Indian Ocean (Bay of Bengal, Haque et al., 2012), the basin experiences less frequent intense tropical storms compared to the West Pacific and North Atlantic, which poses a challenge when assessing changes to storm intensity. A further complication is the sensitivity of storm sure height to non-climate factors such as (along-trajectory) bathymetry (Rahman et al., 2019) for which there are few high-resolution datasets and subject to changes on climate timescales over dynamic delta regions such as the Bay of Bengal. Assessing the contribution to coastal risks from changing storm characteristics is beyond the scope of the present study and represents an area for further research.

Further work is also required to integrate the sea level projections with other information at the local level in order to provide realistic and plausible scenarios of coastal inundation and flooding, and to assess impacts and adaptation options for different sectors. Collaborations with partners in Bangladesh and Pakistan are being pursued in the CARISSA project, building on local information and expertise. Ultimately this work aims to inform regional, national and local climate change adaptation policy and decision-making, and therefore alignment of such work with institutional and government planning is needed to embed the new information in practice.

References

Andrews, T., Gregory, J. M., Webb, M. J., & Taylor, K. E. (2012). Forcing, feedbacks and climate sensitivity in CMIP5 coupled atmosphere-ocean climate models. *Geophysical Research Letters*, *39*(9), n/a-n/a. https://doi.org/10.1029/2012GL051607

Becker, M., Papa, F., Karpytchev, M., Delebecque, C., Krien, Y., Khan, J. U., et al. (2020). Water level changes, subsidence, and sea level rise in the Ganges-Brahmaputra-Meghna delta. *Proceedings of the National Academy of Sciences of the United States of America*, *117*(4), 1867–1876. https://doi.org/10.1073/pnas.1912921117

Brammer, H. (2014). Bangladesh's dynamic coastal regions and sea-level rise. *Climate Risk Management*, *1*, 51–62. https://doi.org/10.1016/J.CRM.2013.10.001

Cannaby, H., Palmer, M. D., Howard, T., Bricheno, L., Calvert, D., Krijnen, J., et al. (2016). Projected sea level rise and changes in extreme storm surge and wave events during the 21st century in the region of Singapore, *12*(3), 613–632. https://doi.org/10.5194/os-12-613-2016

Church, J.A., P.U. Clark, A. Cazenave., J.M. Gregory., S. Jevrejeva., A. Levermann., et al. (2013). *Change 2013: The Physical Science Basis. Contribution of Working Group I to the Fifth Assessment Report of the Intergovernmental Panel on Climate Change* . *Jan Lenaerts*. Jan H. van Angelen.

Church, John A., White, N. J., Konikow, L. F., Domingues, C. M., Cogley, J. G., Rignot, E., et al. (2011). Revisiting the Earth's sea-level and energy budgets from 1961 to 2008. *Geophysical Research Letters*, *38*(18). https://doi.org/10.1029/2011GL048794

Collins, M., Knutti, R., Arblaster, J., Dufresne, J., Fichefet, T., Friedlingstein, P., et al. (2013). *Long-term Climate Change: Projections, Commitments and Irreversibility)*.

Le Cozannet, G., Nicholls, R. J., Hinkel, J., Sweet, W. V., McInnes, K. L., Van de Wal, R. S.

W., et al. (2017). Sea Level Change and Coastal Climate Services: The Way Forward. *Journal of Marine Science and Engineering*, *5*(4), 49. https://doi.org/10.3390/jmse5040049

DeConto, R. M., & Pollard, D. (2016). Contribution of Antarctica to past and future sea-level rise. *Nature*, *531*(7596), 591–597. https://doi.org/10.1038/nature17145

Dieng, H. B., Champollion, N., Cazenave, A., Wada, Y., Schrama, E., & Meyssignac, B. (2015). Environmental Research Letters Total land water storage change over 2003-2013 estimated from a global mass budget approach. *Environ. Res. Lett*, *10*, 124010. https://doi.org/10.1088/1748-9326/10/12/124010

Edwards, T. L., Brandon, M. A., Durand, G., Edwards, N. R., Golledge, N. R., Holden, P. B., et al. (2019). Revisiting Antarctic ice loss due to marine ice-cliff instability. *Nature*, *566*(7742), 58–64. https://doi.org/10.1038/s41586-019-0901-4

Eyring, V., Bony, S., Meehl, G. A., Senior, C. A., Stevens, B., Stouffer, R. J., & Taylor, K. E. (2016). Overview of the Coupled Model Intercomparison Project Phase 6 (CMIP6) experimental design and organization. *Geoscientific Model Development*, *9*(5), 1937–1958. https://doi.org/10.5194/gmd-9-1937-2016

Gregory, J. M., Griffies, S. M., Hughes, C. W., Lowe, J. A., Church, J. A., Fukimori, I., et al. Concepts and Terminology for Sea Level: Mean, Variability and Change, Both Local and Global, 40 Surveys in Geophysics § (2019). Springer Netherlands. https://doi.org/10.1007/s10712-019-09525-z

Griffies, S. M., Yin, J., Durack, P. J., Goddard, P., Bates, S. C., Behrens, E., et al. (2014). An assessment of global and regional sea level for years 1993-2007 in a suite of interannual core-II simulations. *Ocean Modelling*, *78*, 35–89. https://doi.org/10.1016/j.ocemod.2014.03.004

Han, W., Stammer, D., Thompson, P., Ezer, T., Palanisamy, H., Zhang, X., et al. (2019). Impacts of Basin-Scale Climate Modes on Coastal Sea Level: a Review. *Surveys in Geophysics*, 1–49. https://doi.org/10.1007/s10712-019-09562-8

Haque, U., Hashizume, M., Kolivras, K. N., Overgaard, H. J., Das, B., & Yamamoto, T. (2012). Policy & practice Reduced death rates from cyclones in Bangladesh: what more needs to be done? *Bull World Health Organ*, *90*, 150–156. https://doi.org/10.2471/BLT.11.088302

Hawkins, E., & Sutton, R. (2009). The potential to narrow uncertainty in regional climate predictions. *Bulletin of the American Meteorological Society*, *90*(8), 1095–1107.

https://doi.org/10.1175/2009BAMS2607.1

Higgins, S. A., Overeem, I., Steckler, M. S., Syvitski, J. P. M., Seeber, L., & Akhter, S. H. (2014). InSAR measurements of compaction and subsidence in the Ganges-Brahmaputra Delta, Bangladesh. *JOURNAL OF GEOPHYSICAL RESEARCH-EARTH SURFACE*, *119*(8), 1768–1781. https://doi.org/10.1002/2014JF003117

Hinkel, J., Church, J. A., Gregory, J. M., Lambert, E., Le Cozannet, G., Lowe, J., et al. (2019). Meeting User Needs for Sea Level Rise Information: A Decision Analysis Perspective. *Earth's Future*, *7*(3), 320–337. https://doi.org/10.1029/2018EF001071

Howard, T., & Palmer, M. D. (2020). Sea-level rise allowances for the UK. *Environmental Research Communications*, *2*(3), 035003. https://doi.org/10.1088/2515-7620/ab7cb4

Howard, T., Palmer, M. D., & Bricheno, L. M. (2019). Contributions to 21st century projections of extreme sea-level change around the UK. *Environmental Research Communications*, *1*(9), 095002. https://doi.org/10.1088/2515-7620/ab42d7

IPCC. (2019). Special Report on the Ocean and Cryosphere in a Changing Climate — Just another IPCC site. Retrieved May 15, 2020, from https://www.ipcc.ch/srocc/

Jisan, M. A., Bao, S., & Pietrafesa, L. J. (2018). Ensemble projection of the sea level rise impact on storm surge and inundation at the coast of Bangladesh. *Natural Hazards and Earth System Sciences*, *18*(1), 351–364. https://doi.org/10.5194/nhess-18-351-2018

Kahana, R., Abdon, R., Daron, J., & Scannell, C. (2016). *Projections of mean sea level change for the Philippines*.

Knutson, T., Landsea, C., & Emanuel, K. (2012). Tropical Cyclones and Climate Change: A Review (pp. 243–284). https://doi.org/10.1142/9789814293488_0009

Knutti, R., & Hegerl, G. C. (2008, November 26). The equilibrium sensitivity of the Earth's temperature to radiation changes. *Nature Geoscience*. Nature Publishing Group. https://doi.org/10.1038/ngeo337

Kopp, R. E., Gilmore, E. A., Little, C. M., Lorenzo-Trueba, J., Ramenzoni, V. C., & Sweet, W. V. (2019). Usable Science for Managing the Risks of Sea-Level Rise. *Earth's Future*, *7*(12), 1235–1269. https://doi.org/10.1029/2018EF001145

Lahijani, H. A. K., Amjadi, S., Pourkerman, M., Naderi, A., Hosseindoost, M., & Habibi, P. (2019). Makran continental margin sedimentation during the Late Holocene. *CANADIAN JOURNAL OF EARTH SCIENCES*, *56*(6), 629–636. https://doi.org/10.1139/cjes-2018-0087

Landerer, F. W., Gleckler, P. J., & Lee, T. (2014). Evaluation of CMIP5 dynamic sea surface height multi-model simulations against satellite observations. *Climate Dynamics*, *43*(5–6), 1271–1283. https://doi.org/10.1007/s00382-013-1939-x

Levermann, A., Winkelmann, R., Nowicki, S., Fastook, J. L., Frieler, K., Greve, R., et al. (2014). Projecting Antarctic ice discharge using response functions from SeaRISE ice-sheet models, *5*(2), 271–293. https://doi.org/10.5194/esd-5-271-2014

Llovel, W., & Lee, T. (2015). Importance and origin of halosteric contribution to sea level change in the southeast Indian Ocean during 2005-2013. *Geophysical Research Letters*, *42*(4), 1148–1157. https://doi.org/10.1002/2014GL062611

Lowe, J.A, & Gregory, J. . (2005). The effects of climate change on storm surges around the United Kingdom. *Philosophical Transactions of the Royal Society A: Mathematical, Physical and Engineering Sciences*, *363*(1831), 1313–1328. https://doi.org/10.1098/rsta.2005.1570

Lowe, Jason A, Bernie, D., Bett, P., Bricheno, L., Brown, S., Calvert, D., et al. (2018). *UKCP18 Science Overview Report*. Retrieved from www.metoffice.gov.ukwww.metoffice.gov.uk

Lyu, K., Zhang, X., & Church, J. A. (2020). Regional Dynamic Sea Level Simulated in the CMIP5 and CMIP6 Models: Mean Biases, Future Projections, and Their Linkages. *Journal of Climate*, *33*(15), 6377–6398. https://doi.org/10.1175/JCLI-D-19-1029.1

Meehl, G. A., Covey, C., Delworth, T., Latif, M., Mcavaney, B., Mitchell, J. F. B., et al. (2007). THE WCRP CMIP3 MULTIMODEL DATASET A New Era in Climate Change Research. https://doi.org/10.1175/BAMS-88-9-1383

Meinshausen, M., Smith, S. J., Calvin, K., Daniel, J. S., Kainuma, M. L. T. T., Lamarque, J.-F., et al. (2011). The RCP greenhouse gas concentrations and their extensions from 1765 to 2300. *Climatic Change*, *109*, 213–241. https://doi.org/10.1007/s10584-011-0156-z

Nicholls, R. J., & Lowe, J. A. (2004). Benefits of mitigation of climate change for coastal areas. *Global Environmental Change*, *14*(3), 229–244. https://doi.org/10.1016/j.gloenvcha.2004.04.005

Nidheesh, A. G., Lengaigne, M., Vialard, J., Izumo, T., Unnikrishnan, A. S., & Krishnan, R. (2019). Natural decadal sea-level variability in the Indian Ocean: lessons from CMIP models. *Climate Dynamics*, 1–21. https://doi.org/10.1007/s00382-019-04885-z

Oppenheimer, M., & Glavovic, B. (2019). Chapter 4: Sea Level Rise and Implications for Low

Lying Islands, Coasts and Communities. IPCC SR Ocean and Cryosphere. *IPCC Special Report on the Ocean and Cryosphere in a Changing Climate [H.- O. Pörtner, D.C. Roberts, V. Masson-Delmotte, P. Zhai, M. Tignor, E. Poloczanska, K. Mintenbeck, M. Nicolai, A. Okem, J. Petzold, B. Rama, N. Weyer (Eds.)]. In Press.*, *Chapter 4*(Final Draft), 1–14. https://doi.org/10.1126/science.aam6284

Palmer, M., Howard, T., Tinker, J., Lowe, J., Bricheno, L., Calvert, D., et al. (2018). *UKCP18 Marine Report*. Retrieved from www.metoffice.gov.ukwww.metoffice.gov.uk

Palmer, M. D., Gregory, J. M., Bagge, M., Calvert, D., Hagedoorn, J. M., Howard, T., et al. (2020). Exploring the Drivers of Global and Local Sea-Level Change over the 21st Century and Beyond. *Earth's Future*. Retrieved from https://onlinelibrary.wiley.com/doi/abs/10.1029/2019EF001413

Palmer, Matthew D, Harris, G. R., & Gregory, J. M. (2018). Environmental Research Letters Extending CMIP5 projections of global mean temperature change and sea level rise due to thermal expansion using a physically-based emulator. *Environ. Res. Lett*, *13*, 84003. https://doi.org/10.1088/1748-9326/aad2e4

Pardaens, A. K., Gregory, J. M., & Lowe, J. A. (2011). A model study of factors influencing projected changes in regional sea level over the twenty-first century. *Climate Dynamics*, *36*(9–10), 2015–2033. https://doi.org/10.1007/s00382-009-0738-x

Pethick, J., & Orford, J. D. (2013). Rapid rise in effective sea-level in southwest Bangladesh: Its causes and contemporary rates. *Global and Planetary Change*, *111*, 237–245. https://doi.org/10.1016/J.GLOPLACHA.2013.09.019

Pörtner, H., Roberts, D. C., Masson-Delmotte, V., Zhai, P., Tignor, M., Poloczanska, E., et al. (2019). Summary for Policymakers. In: IPCC Special Report on the Ocean and Cryosphere in a changing Climate. *IPCC Report 2019*, (vii, 973), 35. https://doi.org/http://www.ipcc.ch/publications_and_data/ar4/wg2/en/spm.html

Rahman, S., Islam, A. K. M. S., Saha, P., Tazkia, A. R., Krien, Y., Durand, F., et al. (2019). Projected changes of inundation of cyclonic storms in the Ganges–Brahmaputra–Meghna delta of Bangladesh due to SLR by 2100. *Journal of Earth System Science*, *128*(6), 145. https://doi.org/10.1007/s12040-019-1184-8

Rohmer, J., Le Cozannet, G., & Manceau, J. C. (2019). Addressing ambiguity in probabilistic assessments of future coastal flooding using possibility distributions. *Climatic Change*, *155*(1), 95–109. https://doi.org/10.1007/s10584-019-02443-4

Slangen, A. B. A., Carson, M., Katsman, C. A., van de Wal, R. S. W., Köhl, A., Vermeersen,

L. L. A., & Stammer, D. (2014). Projecting twenty-first century regional sea-level changes. *Climatic Change*, *124*(1–2), 317–332. https://doi.org/10.1007/s10584-014-1080-9

Stammer, D., Wal, R. S. W., Nicholls, R. J., Church, J. A., Le Cozannet, G., Lowe, J. A., et al. (2019). Framework for High-End Estimates of Sea Level Rise for Stakeholder Applications. *Earth's Future*, 2019EF001163. https://doi.org/10.1029/2019EF001163

Tamisiea, M., & Mitrovica, J. (2011). The Moving Boundaries of Sea Level Change: Understanding the Origins of Geographic Variability. *Oceanography*, *24*(2), 24–39. https://doi.org/10.5670/oceanog.2011.25

Taylor, K. E., Stouffer, R. J., & Meehl, G. A. (2012, April 1). An overview of CMIP5 and the experiment design. *Bulletin of the American Meteorological Society*. American Meteorological Society. https://doi.org/10.1175/BAMS-D-11-00094.1

Wada, Y., van Beek, L. P. H., Sperna Weiland, F. C., Chao, B. F., Wu, Y.-H., & Bierkens, M. F. P. (2012). Past and future contribution of global groundwater depletion to sea-level rise. *Geophysical Research Letters*, *39*(9), n/a-n/a. https://doi.org/10.1029/2012GL051230

Wada, Y., Lo, M.-H. H., Yeh, P. J. F., Reager, J. T., Famiglietti, J. S., Wu, R.-J. J., & Tseng, Y.-H. H. (2016). Fate of water pumped from underground and contributions to sea-level rise. *Nature Climate Change*, *6*(8), 777–780. https://doi.org/10.1038/nclimate3001

Walsh, K. J. E., Mcbride, J. L., Klotzbach, P. J., Balachandran, S., Camargo, S. J., Holland, G., et al. (2012). Tropical cyclones and climate change. In *Wiley Interdisciplinary Reviews: Climate Change* (Vol. 7, pp. 243–284). https://doi.org/10.1142/9789814293488_0009

Woodruff, J. D., Irish, J. L., & Camargo, S. J. (2013). Coastal flooding by tropical cyclones and sea-level rise. https://doi.org/10.1038/nature12855

ARRCC
Asia Regional Resilience to a Changing Climate

Delivery Partners:

UKaid
from the British people

Met Office